La mer 45 : 69-80, 2007
Société franco-japonaise d'océanographie, Tokyo

Vertical profiles of trace nitrate in surface oceanic waters of the North Pacific Ocean and East China Sea

Jota KANDA[1], Takayuki ITOH[2] and Motomune NOMURA[2]

Abstract: Trace nitrate in surface waters at several stations of the North Pacific Ocean and East China Sea were determined by a high-sensitivity chemiluminescence method. The detailed vertical distribution of nitrate within the surface layer based on water samples taken at small depth intervals revealed that nitrate concentrations were approximately uniform within the euphotic zone, then increased abruptly with depth from the upper end of the nitracline. Nitrate concentrations above the nitracline ranged 3.1–96.2nM, likely reflecting nitrate supply from depths. The depth of the upper end of the nitracline was located at a light depth of 0.58–3.5% at all stations except two, at which the surface mixed layer extended down to the upper end of the nitracline. These depths corresponded closely to the conventional bottom of the euphotic zone, indicating a strong biological control on the nitrate distribution. If the observed nitrate distribution is maintained steadily, net biological nitrate consumption should occur over a narrow depth range near the upper end of the nitracline and no net uptake or regeneration should occur in the upper layers of the euphotic zone.

Keywords: *Nitrate, Vertical profile, Chemiluminescent technique*

1. Introduction

Nitrate in the surface layer of stratified ocean waters is depleted by biological consumption to levels substantially below 100nM. However, as the detection limits of conventional spectrophotometric analysis for nitrate are usually in the range of 100nM (STRICKLAND and PARSONS,1972), alternative techniques capable of much lower detection limits are required. The use of chemiluminescence for high-sensitivity analysis of nitrate (GARSIDE, 1982) revealed the presence of trace nitrate in the low nanomolar range at sites in oligotrophic waters (GARSIDE,1985; EPPLEY and RENGER, 1986). Other high-sensitivity analytical methods are now also in use (OUDOT and MONTEL, 1989; ZHANG, 2000).

These high-sensitivity analytical methods have been used to determine nitrate concentrations in several oceanic domains (e.g. GARSIDE, 1985; EPPLEY and RENGER, 1986; GLOVER *et al.*, 1988; EPPLEY *et al.*, 1990; WOODWARD and OWENS, 1990; MANTOURA *et al.*, 1993; HARRISON *et al.*, 1996; DORE and KARL, 1996a; LIPSCHULTZ, 2001; CAVENDER-BARES *et al.*, 2001; KANDA *et al.*, 2003; CHEN *et al.*, 2004; KROM *et al.*, 2005). However, high-sensitivity measurements of the nitrate distribution remain limited, particularly for the western part of the Pacific Ocean. In the present paper, a modified chemiluminescence technique following GARSIDE (1982) is employed to obtain detailed vertical profiles of nitrate concentration at several sites in the Pacific Ocean and in the waters adjacent to Japan. The obtained results are discussed with regard to the physical structure of the water column and the biological processes relevant to the control of nitrate concentrations. Emphasis is placed on the detailed variation of nitrate near the upper end of the nitracline, where nitrate concentrations begin to increase sharply with depth.

[1] Faculty of Marine Science, Tokyo University of Marine Science and Technology, 4-5-7 Konan, Minato-ku, Tokyo 108-8477, JAPAN
[2] Faculty of Science, Shizuoka University, 836 Ohya, Suruga-ku, Shizuoka-shi, Shizuoka 422-8529, JAPAN

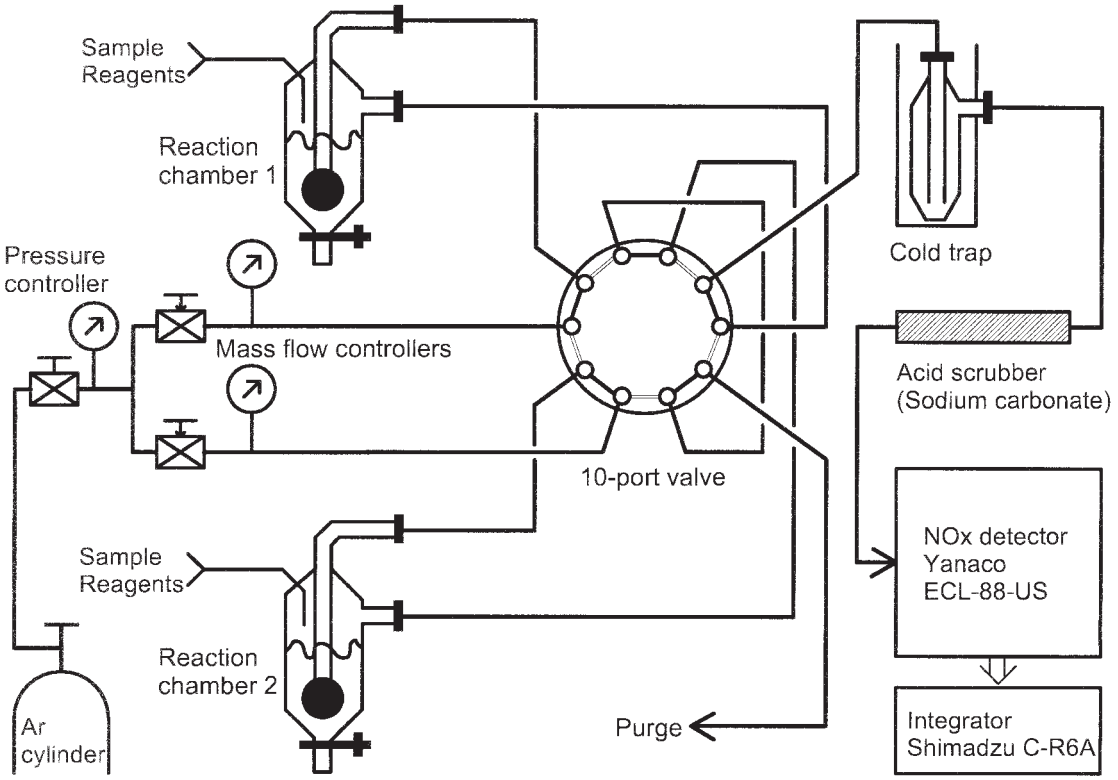

Fig. 1. Schematic diagram of chemiluminescent analysis.

2. Materials and Methods

Nitrate concentrations were determined by the chemiluminescent method of GARSIDE (1982) using the analytical system of COX (1980) and GARSIDE (1982) with modifications to increase the sample processing rate. In the present study, a system with two reaction chambers connected via a 10–port valve is used (Fig. 1). The two chambers are used alternately. The carrier gas (Ar) is supplied from a gas cylinder through two different lines; one line is dedicated strictly for analysis and is connected directly to the chemiluminescent NOx detector, and the other line is used for pre–purging with the mixed reducing reagent. The gas flow in each line is controlled by a pressure regulator and a mass–flow controller.

While the chamber is connected to the pre–purge line, the reducing reagents are introduced successively by dispenser units connected to the chamber in the following order: 10mL sulfuric acid (H_2SO_4, ca. 95%), 2mL 4% (w/v) aqueous ammonium iron (II) sulfate ($Fe(NH_4)_2(SO_4)_2 \cdot 6H_2O$) solution, and 2mL 2% (w/v) aqueous ammonium molybdate ($(NH_4)_2MoO_4$) solution. After pre–purging, the line is switched to the analytical line, and 10mL of the seawater sample is introduced to the chamber by a dispenser unit. The evolved nitrogen monoxide (NO) is lead to a chemiluminescent NOx detector (ECL–88US, Yanaco, Kyoto, Japan), and the peak area of NO concentration is calculated by an integrator (C–R6A, Shimadzu, Kyoto, Japan). The peak area was calibrated in advance against the peak area of standard solutions of known concentrations. Another reaction chamber was pre–purged in preparation for analysis of the following sample during analysis of the current sample. The samples and standards were prepared by adding a 1/50 proportion of 1% sulfanilamide solution. The present analysis thus determines only nitrate, not nitrite (GARSIDE, 1982).

Pure water obtained from a water

Table 1. Station locations and date/time of sampling

Station/Cast	Location	Date	Local Time	Cruise
C	22° 46′N, 158° 07′W	31Oct. 1993	10 : 20	KH–93–4
B CastB10	31° 40′N, 136° 00′E	2Sept. 1995	19 : 10	KT–95–12
CastB12		3Sept. 1995	00 : 10	K–95–09
D4	29° 18′N, 127° 28′E	5Nov. 1995	14 : 21	K–95–09
D6	29° 21′N, 127° 21′E	6Nov. 1995	18 : 42	K–95–09
G2	28° 00′N, 126° 45′E	10Nov.1995	16 : 38	K–95–09
G3	28° 01′N, 126° 43′E	12Nov.1995	11 : 58	K–95–09
G4	28° 04′N, 126° 39′E	13Nov.1995	06 : 37	K–95–09

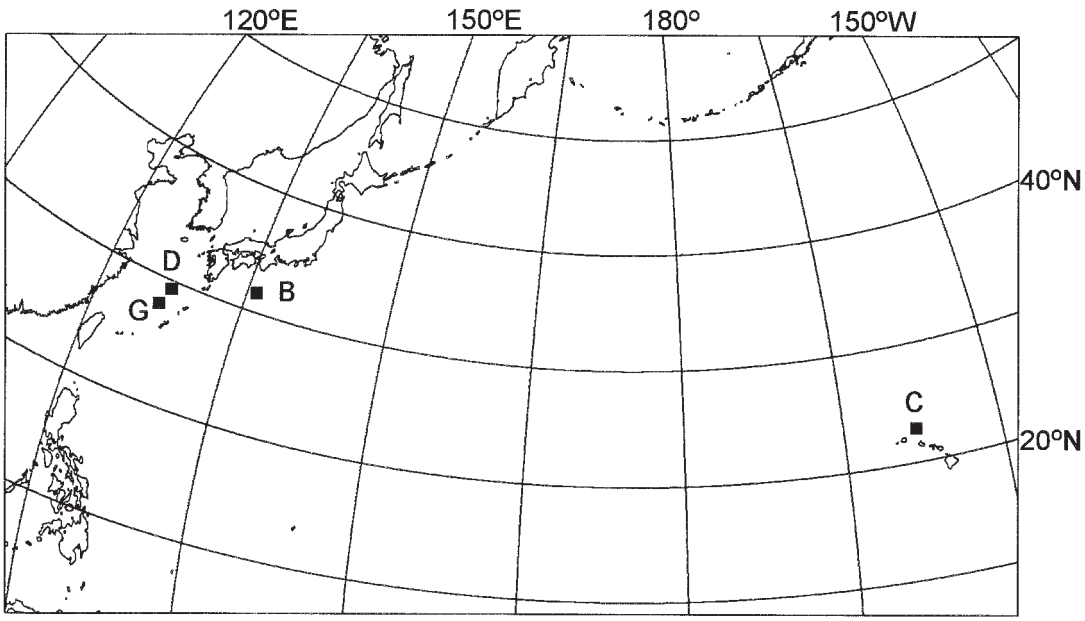

Fig. 2. Station locations.

purification system (Milli–Q Lab, Nihon Millipore, Tokyo, Japan) was used as an analytical blank. The calculated detection limit (y_B+3s_B) for the present analyses is 2.1nM, with reproducibility at 20nM nitrate concentration of 1.8% ($n=10$). All glassware used in the analysis was rinsed with dilute hydrochloric acid solution (ca. 0.05M) and pure water immediately prior to analysis.

Samples for nitrate analysis were obtained during cruises KH–93–4 of the research vessel (R/V) *Hakuho–maru*, KT–95–12 of R/V *Tansei–maru*, and K–95–09 of R/V Kaiyo (Table 1). Vertical profiles were obtained from a total of 8 casts at locations shown in Fig. 2. One profile was obtained at Station C of KH–93–4, which is located off Hawaii in the observational area of Station ALOHA of the Hawaiian Ocean Time–series (KARL and LUKAS, 1996). Station B (KT–95–12) was located in pelagic water south of the Kii Peninsula, Japan, where the 2 casts (B10 and B12) were conducted near sunset and at midnight, respectively. Stations D4, D6, G2, G3 and G6 were in waters off Okinawa, Japan in the shelf–break and trough region of the East China Sea (not on the continental shelf). Stations D4 and D6 were on Line D of the K–95–09 cruise undertaken as part of the MASFLEX project (TSUNOGAI *et al.*, 2003). Stations G2, G3 and G6 were on Line G of the same cruise. These stations were located at intervals of several miles, and only approximate locations are shown (D and G) in Fig. 2. Details of sampling casts are listed in Table 1.

Seawater samples were collected in Niskin bottles using a rosette multi–sampler. Water

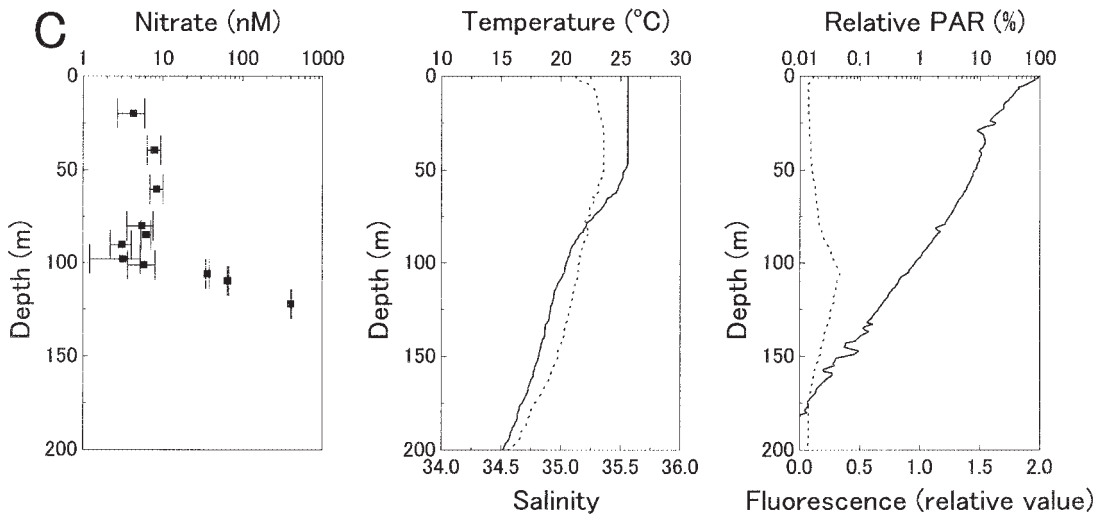

Fig. 3. Vertical profiles of nitrate, temperature, salinity, relative PAR and chlorophyll fluorescence at Station C. Error bars indicate standard deviation of 3 to 8 repeated measurement for one depth sample.

samples were often taken at small depth intervals (down to 5m). While we took care to ascend (descend) the samplers at a rate below ca. 0.3m s^{-1}, possible effect of perturbation by the CTD–sampler system on the observed nitrate distribution should not be precluded. Temperature and salinity profiles were obtained using a Niel–Brown or a Seabird CTD system. Underwater irradiance and chlorophyll fluorescence were observed using either an OCTOPUS system (ISHIMARU et al., 1984) or a natural fluorescence profiler (PNF–300, Biospherical Instruments, San Diego, USA). The underwater irradiance was determined as the photosynthetically available radiation (PAR) scalar irradiance on a quantum basis. The seawater samples were stored frozen until later analysis ashore, except for samples obtained at Station C of KH–93–4, where analysis was performed onboard.

3. Results

Profiles obtained at Station C near Hawaii showed that nitrate concentration ranged from 3.1 to 8.4nM in the upper 100m of the water column and was relatively uniform (Fig. 3). The nitrate concentration at a depth of 101m was 5.8nM, increasing to 36.1 nM at 106m and rising sharply with depth thereafter. The upper end of the nitracline is thus inferred to be located between 101 and 106m. The surface mixed layer was ca. 50m thick, and the temperature and salinity decreased steadily below this level. The maximum chlorophyll fluorescence occurred at 106m, only a few meters from the upper end of the nitracline. The 1% light depth was 97m, and the upper end of the nitracline corresponded to a light depth of 0.58 –0.78%.

At Station B, south of Honshu Island, Japan, two nitrate profiles were obtained at an interval of 5h, and slight differences in the nitrate concentrations and vertical distributions were found (Fig. 4). Nitrate concentrations in the 20 –90m interval of the first cast at dusk (B10) and the 50–95m interval of the second cast at midnight (B12) were in the range of 20.1–23.8nM. The upper end of the nitracline was located at 90–95m at the time of B10 and 95–100m for B12. The nitracline depth was thus slightly deeper at midnight. The nitrate concentration increased with depth except for a slight decrease at a 105m in both casts. CTD observations indicate that the mixed layer at dusk (B10) extended to 32m, while that at midnight (B12) extended to 36m. The isotherm depth was also slightly deeper at midnight; the 22.5 ℃ level occurred at 101m at dusk but at 103m at midnight. Both the chlorophyll maximum and the 1% light depth were located at 101m.

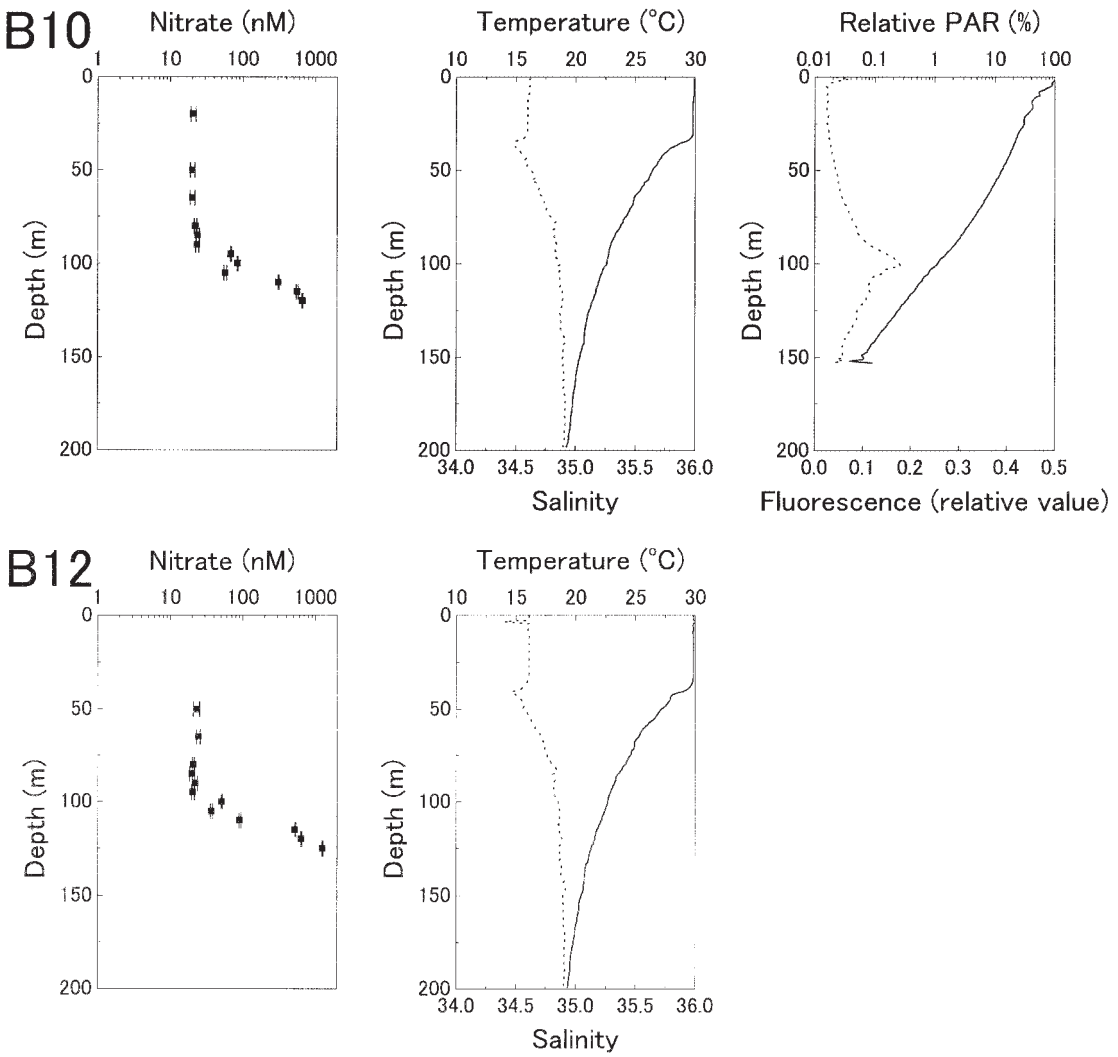

Fig. 4. Vertical profiles of nitrate, temperature and salinity at Station B at dusk (B10, upper) and midnight (B12, lower). Relative PAR and chlorophyll fluorescence were obtained in a separate cast during the daytime (see text).

Note that the observation of chlorophyll fluorescence and underwater irradiance was performed during the daylight hours on the sampling day (Sept. 2, 1995) and thus may not be directly comparable to the profiles observed by the dusk and midnight casts. The upper end of the nitracline (90–100m) was located at a light depth of 1.1–2.1%.

The nitrate concentration in the upper 80m at Station D4 was relatively high, ranging from 35.6 to 96.2nM (Fig. 5). The nitrate distribution was complex. The surface mixed layer extended to a depth of ca. 40m, and another layer with relatively uniform temperature and salinity was found at depths of 60–90m. Both temperature and salinity were lower in this layer, and the nitrate concentration was also relatively low (35–45nM) in the 60–80m. The nitrate concentration increased from 45.1nM at 80m to 531nM at 90m. The 1% light depth was located at 81m, and the upper end of the nitracline (80–90 m) was located at a light depth of 0.64–1.1%. At Station D6, the surface mixed layer was approximately 60m thick, and

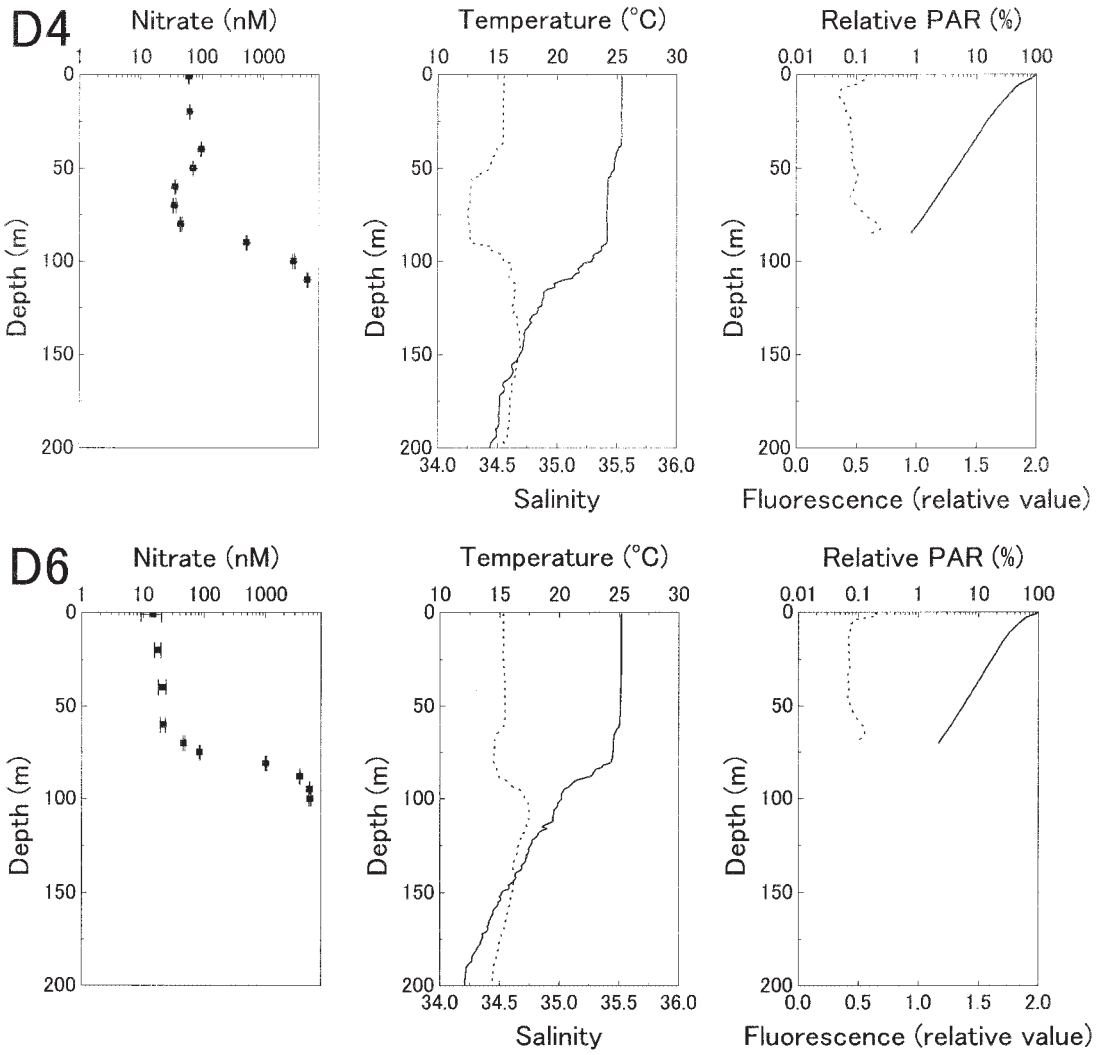

Fig. 5. Vertical profiles of nitrate, temperature, salinity, relative PAR and chlorophyll fluorescence at Stations D4 (upper) and D6 (lower).

a thin layer with uniform temperature and salinity occurred at 70–75m (Fig. 5). The nitrate concentration in the upper 60m of Station D6 was in the range of 14.5–21.3nM. The concentration at 60m was 21.3nM, increasing to 46.3nM at 70m and 83.2nM at 75m. The 1% light depth was outside the observed range of the natural fluorescence profiler, but is inferred by extrapolation to have occurred at a depth of 86m. The upper end of the nitracline (60–70m) corresponded to a light depth of 2.2–3.5%.

At Stations G2, G3 and G6 (Fig. 6), the surface mixed layer extended deeper, reaching 105m, 85m and 100m, respectively. The nitrate concentrations within these mixed layers ranged from 31.5 to 45.9nM at G2, 24.6–25.7nM at G3, and 25.2–47.1nM at G6. The upper end of the nitracline occurred at a depth of 110–120m at G2, 80–90m at G3, and 90–95m at G6. The 1% light depths were about 93m (by extrapolation) at G2, 98m at G3 and 72m at G6. At G2 and G6, the upper end of the nitracline was much deeper than the 1% light depth, where the upper end of the nitracline at G2 (110–120m) corresponded to a light depth of 0.30–

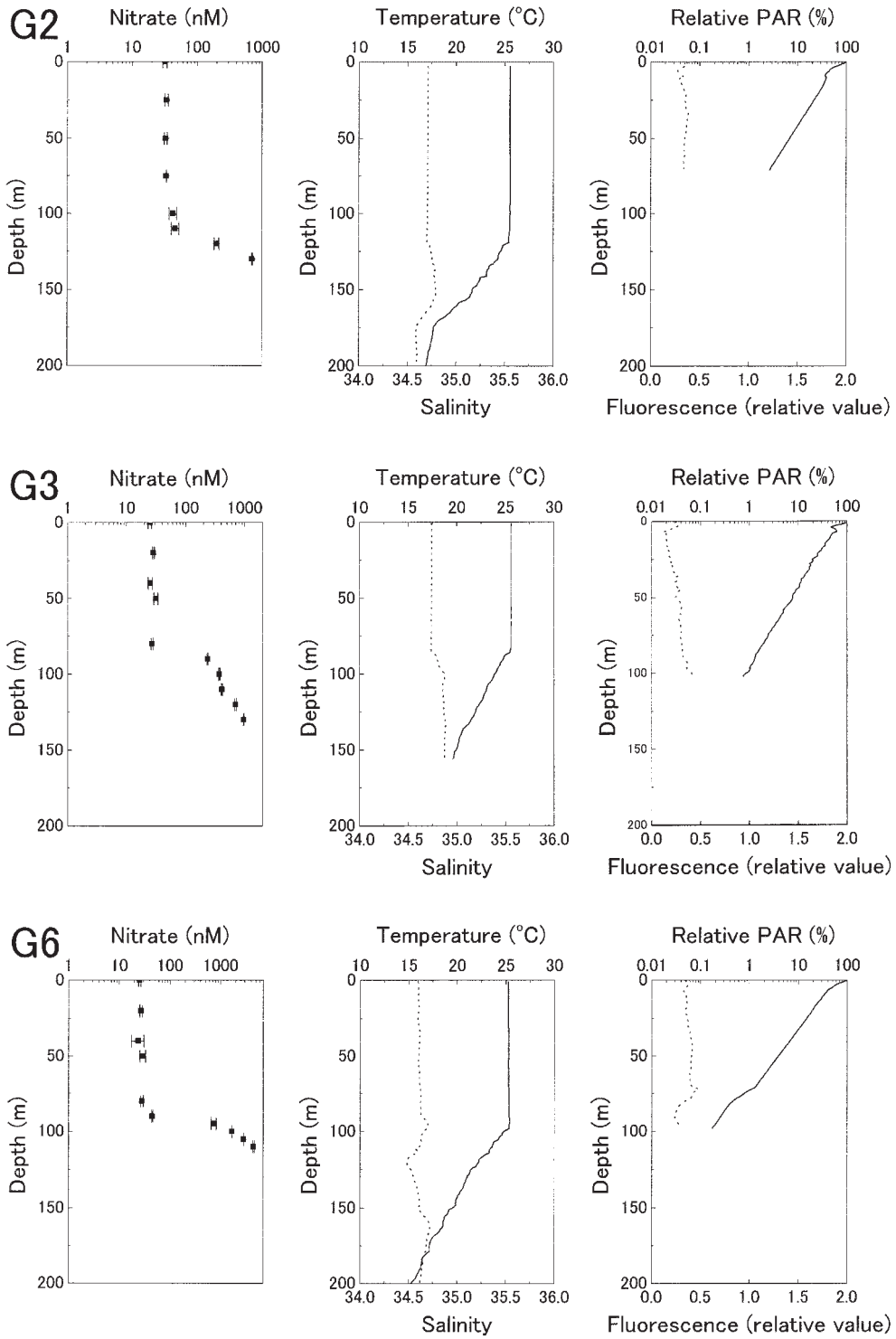

Fig. 6. Vertical profiles of nitrate, temperature, salinity, relative PAR and chlorophyll fluorescence at Stations G2 (upper), G3 (middle) and G6 (lower).

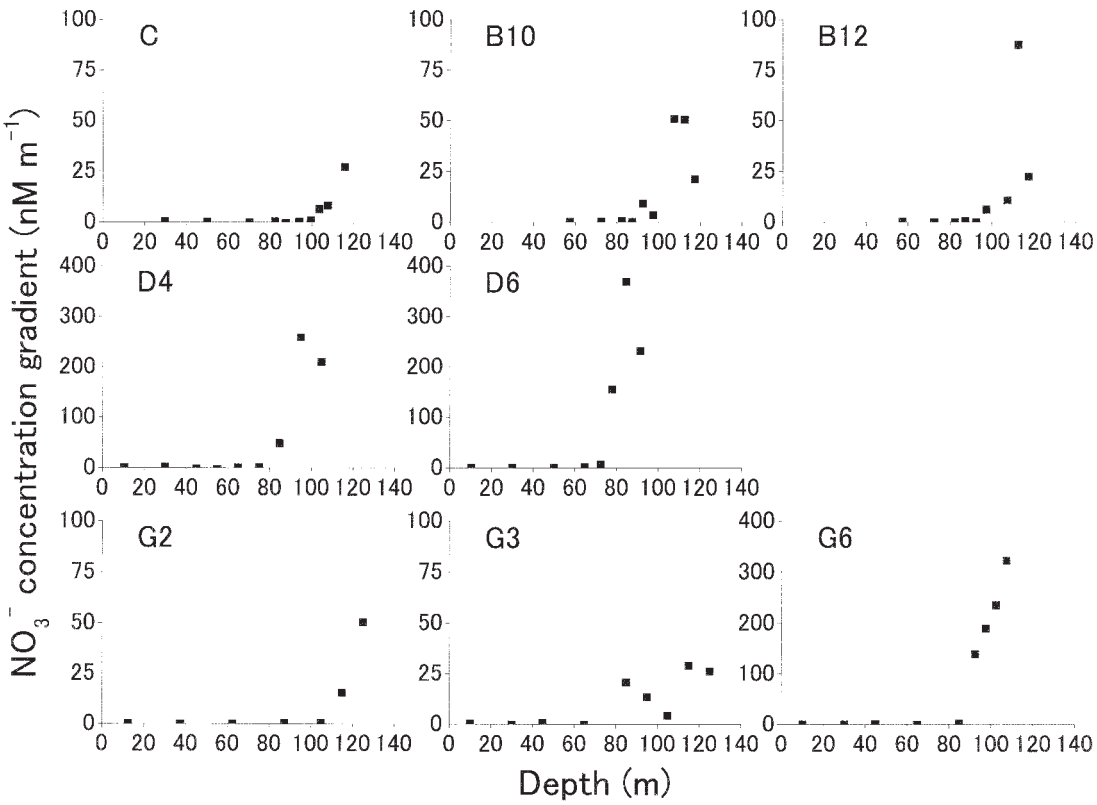

Fig. 7. Variation in nitrate concentration gradient with depth. Difference in nitrate concentration was divided by the depth interval and plotted against the mean depth of two sampling depths. Positive values indicate an increase in concentration with depth.

0.47%, and that at G6 (90–95m) corresponded to a light depth of 0.21–0.26%. In contrast, the upper end of the nitracline at G3 (80–90m) occurred at a light depth of 1.3–2.0%.

4. Discussion

Variation of nitrate concentrations in surface layers

The nitrate concentrations in surface waters of Station C were less than 10nM but still above the detection limit of the present analysis. These low but non–zero values are found consistently at this station in the time series observations of HOT (LETELIER *et al.*, 2000), as well as in other areas of the subtropical oceans (EPPLEY *et al.*, 1990; HARRISON *et al.*, 1996; CAVENDER–BARES *et al.*, 2001). The existence of a threshold concentration of nitrate uptake or a dynamic equilibrium between uptake and regeneration (nitrification) is suggested as possible explanations for these non–zero nitrate concentrations (EPPLEY *et al.*, 1990; MCCARTHY *et al.*, 1992; HARRISON *et al.*, 1996; DORE and KARL, 1996b). At other stations in the present study, nitrate concentrations in surface waters were higher and more variable, likely reflecting the larger supply of nitrate from depth. Under an assumption of simple one –dimensional diffusion, nitrate supply to the euphotic zone is given by the product of the concentration gradient and vertical diffusivity (KING and DEVOL, 1979). Although the temperature and salinity profiles at Station B were similar to those at Station C (Fig. 4), the nitrate concentration gradient within the nitracline was higher (Fig. 7). At Stations D4, D6, G2, G3 and G6, the mixed layer extended deeper, nearly to the nitracline, which may suggest the entrainment of nitrate from such depths (Figs. 5 and 6). The nitrate

concentration gradient at many of these stations was comparable or higher than at Stations B and C (Fig. 7). Higher concentrations are also reported for "nitrate–depleted" waters in the literature, which may similarly be related to the greater supply of nitrate. At the time–series observation site in the subtropical Atlantic Ocean (BATS), nitrate concentrations in winter were high, sometimes exceeding 300nM (LIPSCHULTZ, 2001). This station is located at a higher latitude (31°50′N), and winter–mixing extends much deeper than the euphotic zone. The non–winter concentrations of nitrate were similar to those of stratified subtropical waters. Other observations of higher concentrations have been reported for waters associated with mesoscale eddies (GARSIDE, 1985; ALLEN et al., 1996), wind–induced mixing events (EPPLEY and RENGER, 1988; GLOVER et al., 1988), and possible atmospheric deposition (EPPLEY et al., 1990), as well as in waters of coastal/shelf regions with terrestrial influence and/or a shallower nitracline (EPPLEY and RENGER, 1986; WOODWARD and OWENS, 1990; EPPLEY *et al.*, 1990; CHEN *et al.*, 2004).

Vertical profiles near the upper end of the nitracline

GARSIDE (1985) first described the vertical distribution of trace nitrate in waters around a warm–core ring in the North Atlantic Ocean, where it was found that nitrate concentrations increased exponentially with depth from the surface. EPPLEY *et al.* (1990) also observed a similar exponential increase in nitrate at certain stations, although more typically the nitrate concentrations were found to be relatively uniform within the euphotic zone and to increase abruptly near the bottom of the euphotic zone. This type of profile is more common in other observations in the subtropical oligotrophic Atlantic and Pacific oceans (EPPLEY and KOEVE, 1990; DORE and KARL, 1996a; LIPSCHULTZ, 2001; CAVENDER–BARES *et al.*, 2001). The profiles obtained in the present study all exhibited the latter type of distribution. The upper layer (no concentration gradient) and the nitracline layer (positive concentration gradient) can be clearly separated (Fig. 7).

Based on nitrate data obtained by conventional analytical methods in the equatorial Atlantic Ocean, HERBLAND and VOITURIEZ (1979) suggested that the 1% light depth, chlorophyll maximum and upper end of the nitracline all occur at statistically similar depths. Determination of these depths largely depends on the depth intervals of sampling. In the present study, smaller sampling intervals of 5–10m were adopted for nitrate analysis near the depth of the lower euphotic zone, and the results confirmed that the upper end of the nitracline is associated within a narrow relative PAR range of 0.58–3.5%. Stations G2 and G6 are the exception to this behavior (Fig. 8), where the mixed layer extended much deeper than the 1% light depth. The lower relative PAR recorded at the upper end of the nitracline at these two sites (0.30–0.47% for G2, 0.21–0.26% for G6) should thus be representative of the deep mixed layer. Given the association of nitrate uptake with photosynthetic activity, the occurrence of the upper end of nitracline at similar light–depths indicates a strong biological control on the nitrate distribution.

The maintenance of this type of vertical profiles constrains the vertical variation in the nitrate budget. Assuming the simple one–dimensional diffusive supply of nitrate, the

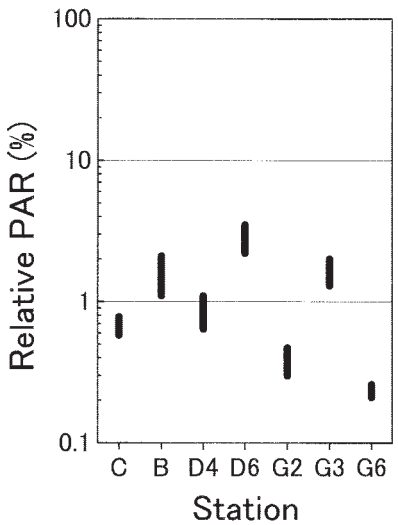

Fig. 8. Estimated depths of upper end of nitracline in terms of relative PAR.

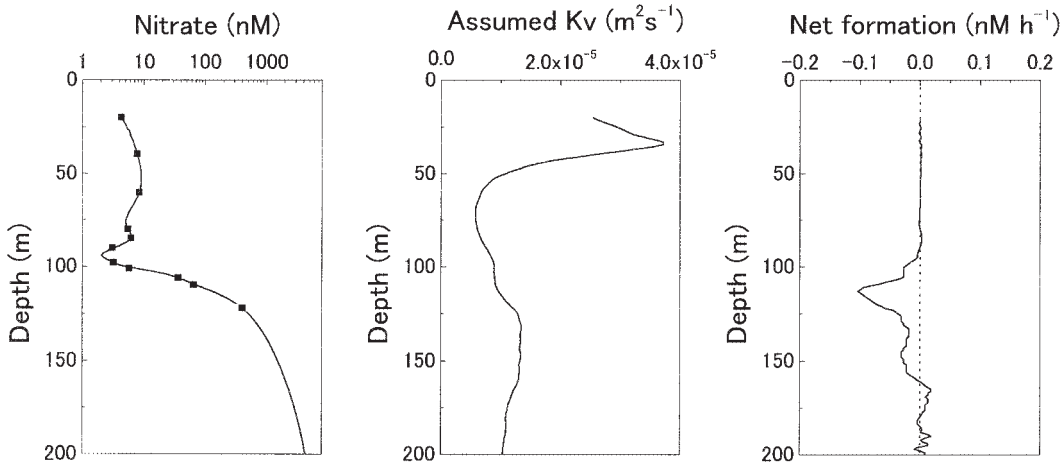

Fig. 9. Interpolated nitrate concentration distribution, assumed vertical diffusivity and estimated net formation/uptake (formation for positive values) of nitrate at Station C.

temporal change of the nitrate concentration (C) at depth z, or the time (t) derivative of C, can be equated with the depth derivatives of C, the vertical diffusivity at depth z [$K_v(z)$] and biological uptake and regeneration of nitrate:

$$\frac{\partial C}{\partial t} = \frac{\partial}{\partial z}\left(K_v(z)\frac{\partial C}{\partial z}\right) - (uptake) + (regeneration) \quad (1)$$

The net biological uptake of nitrate, or the negative value of the net biological formation, should be given as the difference between the uptake and regeneration.

$$(net\ biological\ uptake) = -(net\ biological\ formation) = (uptake) - (regeneration) \quad (2)$$

If the nitrate concentration is in a steady state, the time derivative of C in Equation (1) equals zero, and the net biological uptake is given as

$$(net\ biological\ uptake) = \frac{\partial}{\partial z}\left(K_v(z)\frac{\partial C}{\partial z}\right) \quad (3)$$

The vertical diffusivity at depth z is assumed to be a function of buoyancy frequency or N (GARGETT 1984) as follows.

$$K_v(z) = a_0 N^{-1} \quad (4)$$

An arbitrary value of $1.0\times10^{-7}\mathrm{m^2s^{-1}}$ is assigned for the constant a_0. The resultant vertical distribution of the net biological uptake of nitrate at Station C (Fig. 9) indicates that high net uptake should occur over a narrow depth range near the upper end of the nitracline, whereas no net uptake or formation should occur in the upper layers of the euphotic zone. If plankton populations in these layers utilize nitrate as a nitrogen source, the uptake of nitrate should be in balance with the *in situ* supply of nitrate, or biological regeneration (presumably nitrification) and/or an alternative external supply such as atmospheric deposition.

Acknowledgements

The authors thank the scientists, officers and crewmembers onboard the relevant cruises of the R/V *Hakuho-maru*, R/V *Tansei-maru* and R/V *Kaiyo*. Field observations onboard R/V *Kaiyo* were conducted as a part of the MASFLEX project. This study was supported by Grants-in-Aid from the Ministry of Education, Culture, Sports, Science and Technology of Japan (Nos. 04232206, 04740355, 05216203, 06740420 and 07640655).

References

ALLEN, C.B., J. KANDA and E.A. LAWS (1996): New production and photosynthetic rates within and outside a cyclonic mesoscale eddy in the North Pacific subtropical gyre. Deep-Sea Res. I, **43**, 917–936.

CAVENDER-BARES, K.K., D.M. KARL and S.W. CHISHOLM (2001): Nutrient gradients in the western North Atlantic Ocean: Relationship to

microbial community structure and comparison to patterns in the Pacific Ocean. Deep–Sea Res. I, **48,** 2373–2395.

CHEN, Y.L.L., H.Y. CHEN, D.M. KARL and M. TAKAHASHI (2004): Nitrogen modulates phytoplankton growth in spring in the South China Sea. Continental Shelf Res., **24**, 527–541.

COX, R.D. (1980): Determination of nitrate and nitrite at the part per billion level by chemiluminescence. Anal. Chem., **52**, 332–335.

DORE, J.E. and D.M. KARL (1996a): Nitrite distributions and dynamics at Station ALOHA. Deep–Sea Res. II, **43**, 385–402.

DORE, J.E. and D.M. KARL (1996b): Nitrification in the euphotic zone as a source for nitrite, nitrate and nitrous oxide at Station ALOHA. Limnol. Oceanogr., **41**, 1619–1628.

EPPLEY, R.W., C. GARSIDE, E.H. RENGER and E. ORELLANA (1990): Variability of nitrate concentration in nitrogen–depleted subtropical surface waters. Mar. Biol., **107**, 53–60.

EPPLEY, R.W. and W. KOEVE (1990): Nitrate use by plankton in the eastern subtropical North Atlantic, March–April 1989. Limnol. Oceanogr., **35**, 1781–1788.

EPPLEY, R.W. and E.H. RENGER (1986): Nitrate–based primary production in nutrient–depleted surface waters off California. Oceanographie Tropicale, **21**, 229–238.

EPPLEY, R.W. and E.H. RENGER (1988): Nanomolar increase in surface layer nitrate concentration following a small wind event. Deep–Sea Res., **35**, 1119–1125.

GARGETT, A.E. (1984): Vertical eddy diffusivity in the ocean interior. J. Mar. Res., **42**, 359–393.

GARSIDE, C. (1982): A chemiluminescent technique for the determination of nanomolar concentrations of nitrate and nitrite in seawater. Mar. Chem., **11**, 159–167.

GARSIDE, C. (1985): The vertical distribution of nitrate in open ocean surface water. Deep–Sea Res., **32**, 723–732.

GLOVER, H.E., B.P. PRÉZELIN, L. CAMPBELL, M. WYMAN and C. GARSIDE (1988): A nitrate–dependent bloom in surface Sargasso Sea water. Nature, **331**, 161–163.

HARRISON, W.G., L.R. HARRIS and B.D. IRWIN (1996): The kinetics of nitrogen utilization in the oceanic mixed layer: Nitrate and ammonium interactions at nanomolar concentrations. Limnol. Oceanogr., **41**, 16–32.

HERBLAND, A. and B. VOITURIEZ (1979): Hydrological structure analysis for estimating the primary production in the tropical Atlantic ocean. J. Mar. Res., **37**, 87–101.

ISHIMARU, T., H. OTOBE, T, SAINO, H. HASUMOTO and T. NAKAI (1984):.OCTOPUS, an octo parameter underwater sensor, for use in biological oceanography studies. J. Oceanogr. Soc. Japan, **40**, 207–212.

KANDA, J., T. ITOH, D. ISHIKAWA and Y. WATANABE (2003): Environmental control of nitrate uptake in the East China Sea. Deep–Sea Res. II, **50**, 403–422.

KARL, D.M. and R. LUKAS (1996): The Hawaii Ocean Time–series (HOT) program: Background, rationale and field implementation. Deep–Sea Res. II, **43**, 129–156.

KING, F.D. and A.H. DEVOL (1979): Estimates of vertical eddy diffusion through the thermocline from phytoplankton nitrate uptake rates in the mixed layer of the eastern tropical Pacific. Limnol. Oceanogr., **24**, 645–651.

KROM, M.D., E.M.S. WOODWARD, B. HERUT, N. KRESS, P. CARBO, R.F.C. MANTOURA, G. SPYRES, T.F. THINGSTAD, P. WASSMANN, C. WEXELS–RISER, V. KITIDIS, C.S. LAW and G. ZODIATIS (2005): Nutrient cycling in the south east Levantine basin of the eastern Mediterranean: Results from a phosphorus starved system. Deep–Sea Res. II, **52**, 2879–2896.

LETELIER, R.M., D.M. KARL, M.R. ABBOTT, P. FLAMENT, M. FREILICH, R. LUKAS and T. STRUB (2000): The role of late winter meso–scale events in the biogeochemical variability of the upper water column of the North Pacific Subtropical Gyre. J. Geophys. Res., **105**, 28,723–28,739.

LIPSCHULTZ, F. (2001): A time–series assessment of the nitrogen cycle at BATS. Deep–Sea Res. II, **48**, 1897–1924.

MANTOURA, R.F.C., C.S. LAW, N.J.P. OWENS, P.H. BURKILL, E.M.S. WOODWARD, R.J.M. HOWLAND and C.A. LLEWELLYN (1993): Nitrogen biogeochemical cycling in the northwestern Indian Ocean. Deep–Sea Res. II, **40**, 651–671.

MCCARTHY, J.J., C. GARSIDE and J.L. NEVINS (1992): Nitrate supply and phytoplankton uptake kinetics in the euphotic layer of a Gulf Stream warm–core ring. Deep–Sea Res., **39**, S393–S403.

OUDOT, C. and Y. MONTEL (1988): A high sensitivity method for the determination of nanomolar concentrations of nitrate and nitrite in seawater with a Technicon AutoAnalyzer II. Mar. Chem., **24**, 239–252.

STRICKLAND, J.D.H. and T.R. PARSONS (1972): A Practical Handbook of Sea Water Analysis, 2nd edition. Bulletin of Fisheries Research Board of Canada, **167**, 1–310.

TSUNOGAI, S., K. ISEKI, M. KUSAKABE and Y. SAITO (2003): Biogeochemical cycles in the East China Sea: MASFLEX program. Deep–Sea Res. II, **50**, 321–326.

WOODWARD, E.M.S. and N.J.P. OWENS (1990): Nutrient depletion studies in offshore North Sea

areas. Netherlands J. Sea Res., **25**, 57–63.
ZHANG, J.–Z. (2000): Shipboard automated determination of trace concentrations of nitrite and nitrate in oligotrophic water by gas–segmented continuous flow analysis with a liquid waveguide capillary flow cell. Deep–Sea Res. I, **47**, 1157–1171.

Received June 8, 2007
Accepted July 9, 2007

La mer 45 : 81-90, 2007
Société franco-japonaise d'océanographie, Tokyo

Fluorescent labelling of cultivated corals as a sustainable management tool in coral trade and reefs conservation

Virginie VAN DONGEN-VOGELS* and Jérôme MALLEFET

Abstract: Scleractinian corals are part of an important growing lucrative market trade, which is primarily focused on wild-caught corals. Improving trade regulations and developing asexual/sexual reproduction programmes in aquaria to decrease the pressure exerted on wild populations may require labelling systems to certify coral origin (cultured *vs.* wild-caught). We investigated a simple labelling method based on calcein incubation using 81 coral fragments of six cultivated coral species of two different growth forms (branched and foliaceous). We tested two calcein concentrations (0.01 and 0.02 g l^{-1}) and three incubation times (12, 24 and 36 hours) to determine optimal labelling conditions. The labelling visibility on fragments was assessed 8, 12 and 16 weeks following the incubations. Respectively 59, 61, 79, 96, and 98 % of the calcein incubated-fragments were successfully labelled for *S. caliendrum, Echinopora* sp., *T. reniformis, P. damicornis*, and *S. pistillata and Montipora* sp. While the quality and the durability of the label varied between species, both were significantly improved at the longest incubations for both calcein concentration tested. The relevance of the calcein technique in labelling cultivated corals is discussed in relation to other potential labelling methods and as a sustainable management in coral trade and reef conservation.

Keywords: *Scleractinian, calcein, coral labelling, coral trade, CITES*

1. Introduction

The impacts of anthropogenic activities on coral reefs have been widely reported in the literature and include processes such as eutrophication, oil pollution, tourism expansion, trampling, dredging, overfishing, and cyanide fishing (e.g. SHUMAN *et al.*, 2004 : WILKINSON, 2004 : FABRICIUS, 2005).

Scleractinian corals have also been the focus of a lucrative and constantly growing trade (GREEN and SHIRLEY, 1999 : GREEN and HENDRY, 1999 : FOLKE *et al.*, 2000 : BRUCKNER, 2000, 2001 : DELBEEK, 2001 : WABNITZ *et al.*, 2003). Despite the development and improvement of maintenance and husbandry techniques, less than one percent of the total trade in hard corals is derived from cultured corals (GREEN and SHIRLEY, 1999). Since 1983, international trade of more than 2000 species of corals has been monitored and regulated under the Convention on International Trade in Endangered Species (CITES). All traded coral species are now listed in Appendix II of CITES and then require an export permit from the country of origin, along with proofs that a specimen was legally obtained and that the export will not harm the survival of that species. Countries are required to publish export quotas showing the amount of coral that can be collected and traded each year (GREEN and HENDRY, 1999 : BRUCKNER, 2001 : http://www.cites.org, July 2005). Different environmental agreements, programmes, partnerships, networks, non governmental and governmental organisations have been working to protect and conserve coral reefs (UNEP, 2003) with for instance, the creation of Marine Protected Areas (MPA) where fishing or collecting activities are strictly banned.

Although CITES legislation is strict (GREEN and HENDRY, 1999 : BRUCKNER, 2001), illegal or unreported fishing and coral collecting

Laboratory of Marine Biology, Catholic University of Louvain (UCL), Batiment Kellner, 3 Place Croix du Sud, 1348 Louvain-La-Neuve, Belgium

* Corresponding author
E-mail: virgvdv@yahoo.fr

activities (e.g. HANFEE, 1997 : GREEN and SHIRLEY, 1999 : ISHIHARA, 2000 : TEO, 2005) as well as unreported export/import of live corals are still current. The illegal trade of corals on the black market is one of the greatest concerns in the conservation and protection of coral reefs. In addition, intensive coral collecting activities greatly reduce the percentage of coral cover (e.g. HARRIOTT, 2002 : BRUCKNER and BORNEMAN, 2005) hence affecting the entire reef ecosystem; e.g. up to 70 % of the total reef cover have been reduced in only one decade in the Philippines (GREEN and SHIRLEY, 1999). It is therefore necessary to improve trade regulations in order to minimize coral reef decline. Development of aquaculture facilities for coral propagation in aquarium by both asexual and sexual reproduction (e.g. DELBEEK, 2001 : PETERSON *et al.*, 2006) could allow pressure to be reduced on wild populations, but should require labelling systems which may guarantee coral proveniences (cultivated vs. wild–caught) and help tracking coral in trade. In March 2004, the Permanent Comity of the CITES raised the question regarding the identification of a labelling system for hard corals, which would help to differentiate cultivated from wild–caught corals (SC50 Doc. 10.1. Convention of the International Trade on Endangered Species, 50th session of the Permanent Comity, Geneva, 2004). Furthermore, the Marine Aquarium Council (MAC) has launched an international certification scheme providing security on the traded organisms with the idea of a sustainable management of the reef and the market trade (SHUMAN *et al.*, 2004 : http://www.aquariumcouncil.org, December 2006). In particular, the assessment of labelling methods to distinguish wild–caught from cultured corals requires further investigations as it could lead to the development of a sustainable tool for more consistent monitoring of the coral trade market.

Internal fluorescent markers such as calcein (2, 4 – bis – [N, N' – di (carboxymethyl) – aminomethyl]– fluorescein) are easy to apply, cost effective (i.e. a large number of individuals can be marked in a short time with minimum handling) and can last for several weeks (LEIPS *et al.*, 2001 : THORROLD *et al.*, 2002). Calcein has been used as an efficient marker for both identification and growth measurements (BERNHARD *et al.*, 2004) in various invertebrates such as sponges (ILAN *et al.*, 1996), sclerosponges (WILLENZ and HARTMAN, 1999), gastropods (MORAN, 2000), bivalves (DAY *et al.* 1995, KAEHLER and MCQUAID , 1999) and echinoderms (RUSSEL and MEREDITH , 2000 : RUSSEL and URBANIAK , 2004). Recently, MARSCHAL *et al.* (2004) used calcein as a new method to measure the growth and age of the Mediterranean gorgonian, *Corallium rubrum* (commonly referred to as 'red coral'). Calcein is a fluorescein complex which binds to calcium and is therefore incorporated into growing calcium carbonate structures (BERNHARD *et al.*, 2004) without affecting the growth of the stained individual. Furthermore, when compare to other stains such as alizarin red S or tetracycline calcein appears to be more suitable for staining invertebrates (e.g. DODGE *et al.*, 1984 : DAY *et al.*, 1995). Once bound to calcium, calcein fluoresces and becomes detectable when exposed under ultraviolet light.

In this context, the objectives of this work was to develop a simple calcein–based method for labelling cultivated coral species, thus introducing the idea of a 'conservation label' for traded hard corals. More specifically, using 6 species of branched and foliaceous corals we investigated (i) the optimal labelling conditions necessary to obtain a visible and long lasting mark, (ii) the potential effect of calcein on fragment growth, and (iii) the inter–specific variability in the labelling efficiency.

2. Material and Methods

2.1. Species

The two main families of stony corals traded internationally are Acroporidae and Pocilloporidae (GOMEZ *et al.*, 1985 : WABNITZ *et al.*, 2003). The six species of scleractinian corals considered in the present work have been specifically chosen as they are listed in Appendix II of CITES, known to grow well in aquarium and to reach rapidly a commercial size (GREEN and SHIRLEY, 1999 : DELAHAYE , 2003) and as such can be thought as being representative species for aquarium trade. Three branched Pocilloporidae species (Stylophora pistillata,

Seriatopora caliendrum, and Pocillopora damicornis) and one foliaceous Acroporidae (Montipora sp.) were considered. Two other foliaceous species of Faviidae (Echinopora sp.) and Dendrophylliidae (Turbinaria reniformis) were investigated in order to ensure the generality and relevance of the present work.

2.2. Cutting and handling

For each species, small coral fragments of about 5 cm in length for the branched species and a diameter of about 5 cm for the foliaceous species were obtained from cultivated colonies using a pair of pliers. Tags attached by a thin plastic cable were used to identify each fragment. Fragments of the each species were placed on separate PVC plates and separated from each other to avoid any interaction. Holding plates were then transferred in four 800 l aquaria filled with biologically filtered seawater and fitted with a circulating pump (Eheim 1060, 1200 l h–1), allowing sufficient water flow to support coral growth. Light (300 μE cm–2 s–1) was provided by two m*et al* halide lamps (HQI) located one meter above each aquarium. The temperature was maintained at 26.5–27.5 °C during the entire study.

2.3. Calcein labelling

The labelling experiment consisted in six different incubating conditions carried out in order to infer an optimal condition for obtaining a visible and long lasting mark on coral fragments. Calcein concentrations of 0.01 g l^{-1} to more than 0.60 g l^{-1} (e.g. KAELHER and MCQUAID , 1999 : RUSSELL and MEREDITH, 2000) have been used to stain various invertebrates without affecting their survival. Given the calcein concentrations used by MARSCHAL *et al.* (2004) to stain a gorgonian coral, two calcein solutions (0.01 g l^{-1} and 0.02 g l^{-1}) were prepared according to MORAN (2000). Coral fragments of each species were then removed from the 800 l aquaria and incubated in 50 l aquaria without calcein (control), and with calcein at 0.01 g l^{-1} and 0.02 g l^{-1} for 12, 24, or 36 hours. After incubation, fragments were returned to the 800 l culture aquaria. The 50 l glass aquaria were filled with the same seawater of the 800 l aquaria and their temperature maintained at 26.5–27.5 °C for the duration of the incubations.

Calcein–incubated fragments were subsequently observed one by one under ultraviolet light (UV lamp: 365 nm) for less than one minute. Four mark quality indexes were defined according to the different calcein fluorescence intensity levels (FIL) observed (1 = no mark or absence of calcein : 2 = detectable but faint mark : 3 = bright mark : 4 = very bright mark). The remaining in the visibility of the label on the fragment skeleton was assessed by repeating the observation under the UV lamp 8, 12, and 16 weeks after the first incubations.

2.4. Coral growth

The fragment growth or increase in weight (g) was estimated to the nearest 0.1 g at each time interval of the study (after 12, 24, and 36 hours of calcein incubation, and 8, 12, and 16 weeks later). Coral fragments were taken out of the aquariums and put on a tray for five minutes before weighing them to allow excess water to drain away (DELAHAYE , 2003).

2.5. Statistical analysis

The effects of calcein concentration (g l^{-1}), incubation time (hours), durability of the label over time (weeks), and the inter–species variation on calcein mark readability observed in fragments were tested using ordinal logistic regressions (SAS Enterprise Guide® V2). In order to test for the effect of calcein concentration on fragment growth, we performed for each species a one–way analysis of variance (ANOVA) on the relative weigh increase (in %) of fragments over time. Parametric testing was possible as both the normality and the Levene and Bartlett' s tests for homogeneity of variance were satisfied ($p > 0.05$).

3. Results

After 12, 24, or 36 hours of incubation in calcein concentration of 0.01 or 0.02 g l^{-1}, more than 59 % of all incubated–fragments of each studied species showed a faint, bright or very bright yellow–green fluorescent mark when observed under the UV lamp. The mark was readily distinguished from naturally occurring

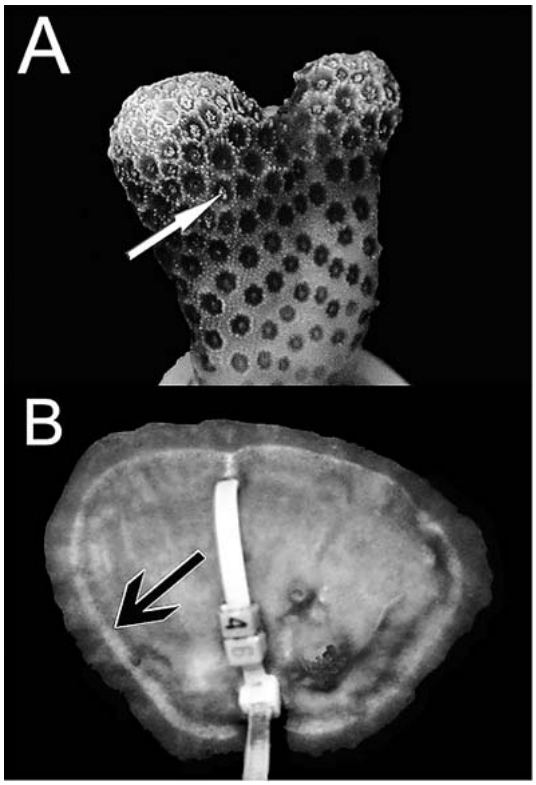

Fig. 1. Illustration of fluorescent labelled-fragments observed under ultraviolet-light. A: Calcein fluorescence observed immediately after incubation on a fragment of S. pistillata and easily differentiated from the polyps auto-fluorescence (white arrow). B: A calcein fluorescent band (black arrow) easily observed on the shaded part of a fragment of T. reniformis 8 weeks after incubation.

auto fluorescence by comparing calcein–incubated fragments with the controls (Fig. 1). The mean FIL obtained for both experiments are given in Table 1. They give information on the amount but especially on the quality of the marks obtained (DAY *et al.*, 1995). In addition, the evolution of the percentage of labelled–fragments obtained from incubations is represented for each species in Fig. 2. This percentage is considered to be easier to picture and it provides a better idea of the reliability of the method; i.e. < 50 % of labelled–fragments will mean that the conditions used in this study are thus not reliable for a labelling system, 50 to 80 %: the method can potentially be reliable but the conditions need to be reviewed, > 80 %: the method is reliable but may need to be improved.

3.1. Optimal conditions after incubations and inter–species variation

Firstly, we determined whether a condition of incubation would be more suitable (i.e. higher marking scores obtained) for each species separately. While an effect of the incubation time was significantly showed for fragments of *S. caliendrum* ($p < 0.05$) with higher scores obtained from 36 hours of incubation, no effect of the incubation time was showed for the other species ($p > 0.05$). For each species, both the effect of the incubation time on the FIL and the mean FIL obtained were not influenced by the calcein concentrations ($p > 0.05$). Secondly, we found that decreasing the incubation time (e.g. 24 or 12 hours) led to significant variations in the obtained FIL between species ($p < 0.05$) for both calcein concentrations. While *P. damicornis, Montipora* sp. and *S. pistillata* did not show any significant difference in their FIL, they were all significantly higher than those of *T. reniformis* ($p < 0.05$), and which ones were found significantly higher than *S. caliendrum* and *Echinopora* sp. ($p < 0.05$). These trends are well reflected by the percentage of labelled–fragments obtained after all incubations. Respectively 59, 61, 79, 96, and 98 % of the calcein incubated–fragments were successfully labelled for *S. caliendrum, Echinopora* sp., *T. reniformis, P. damicornis*, and *S. pistillata* and *Montipora* sp.

3.2. Persistence of the label and inter–species variation

The percentage of labelled–fragments of each species significantly decreased over the course of the study ($p < 0.05$), in particular between the first observation following the incubations and the second observation performed 8 weeks later (Fig. 2). However, some species were observed to "lose" the brightness of their label faster than others. For example, while 8 weeks after all conditions of incubation no more marks were visible on the skeleton of the fragments of *S. caliendrum* (Table 1), there were

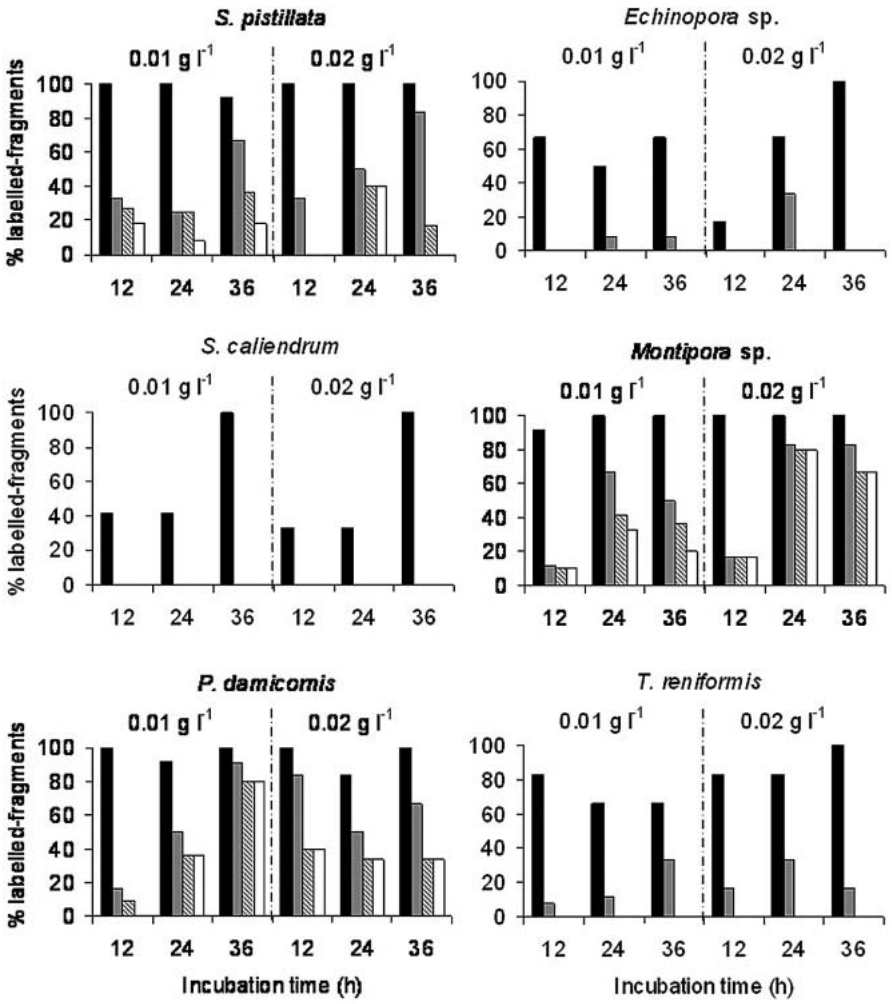

Fig. 2. Temporal evolution of the percentage of labelled-fragments obtained after incubation of each species in calcein at different concentrations (0.01 and 0.02 g l^{-1}) and different incubation times (12, 24, and 36 h). Black: immediately after incubation, grey: 8 weeks after incubation, grey stripes: 12 weeks after incubation, white: 16 weeks after incubation.

still more than 50 % (up to 90 %) of labelled–fragments of *P. damicornis* for most of the condition tested (Table 1). Again, 8 weeks following all incubations, the FIL were not significantly different between *P. damicornis, Montipora* sp. and *S. pistillata*, but were significantly different between these three species and *T. reniformis* and *Echinopora* sp ($p < 0.05$). *T. reniformis* significantly showed higher FIL than *Echinopora* sp. ($p < 0.05$). Twelve weeks after the incubations no marks could be detectable in all fragments skeleton of *Echinopora* sp. and *T. reniformis*. In contrast, the three other species commonly remained a weak percentage (less than 40 %) of labelled–fragments that gradually decreased over the next weeks (Fig. 2). No significant difference in their FIL was showed 12 and 16 weeks after incubations ($p > 0.05$).

Apart from *S. caliendrum, Echinopora* sp. and *T. reniformis*, fragments of the other species studied significantly showed a higher probability to keep a visible mark with higher FIL if incubated for 24 and/or 36 hours ($p > 0.05$).

Table 1. Fluorescent intensity levels (FIL) obtained for different coral species immediately after calcein incubations and 8, 12 and 16 weeks after incubations for each concentration and incubation time tested. Mean ± Standard deviation; n: sample size.

Species	Cone. (g. 1^{-1})	Time (weeks)	12h	n	24h	n	36h	n
S. pistillata	0.01	0	3.3±0.9	12	3.9±0.3	12	3.7±0.9	12
		8	1.3±0.5	12	1.5±1.0	12	1.8±0.7	12
		12	1.3±0.5	11	1.4±0.8	12	1.4±0.5	11
		16	1.2±0.4	11	1.1±0.3	12	1.2±0.4	11
	0.02	0	3.5±0.8	6	3.5±0.8	6	4.0±0.0	6
		8	1.3±0.5	6	1.7±0.8	6	2.3±0.8	6
		12	1.0±0.0	6	1.6±0.9	5	1.2±0.4	6
		16			1.6±0.9	5	1.0±0.0	6
S. caliendrum	0.01	0	1.6±0.9	12	1.9±1.2	12	3.9±0.3	12
		8	1.0±0.0	6	1.0±0.0	11	1.0±0.0	12
	0.02	0	1.7±1.2	6	2.0±1.6	6	3.5±0.8	6
		8	1.0±0.0	6	1.0±0.0	5	1.0±0.0	6
P. damicornis	0.01	0	3.6±0.5	12	3.6±0.9	12	4.0±0.0	12
		8	1.3±0.6	12	1.7±0.8	12	3.3±1.1	11
		12	1.1±0.3	11	1.4±0.5	11	2.2±0.8	10
		16	1.0±0.0	11	1.4±0.5	11	2.1±0.7	10
	0.02	0	3.8±0.4	6	3.3±1.2	6	3.8±0.4	6
		8	2.3±1.0	6	1.7±0.8	6	1.8±0.8	6
		12	1.4±0.6	5	1.3±0.5	6	1.3±0.5	6
		16	1.4±0.6	5	1.3±0.5	6	1.3±0.5	6
Echinopora sp.	0.01	0	1.8±0.6	12	2.2±1.4	12	2.2±1.2	12
		8	1.0±0.0	12	1.3±0.6	12	1.1±0.3	12
		12			1.0±0.0	12	1.0±0.0	11
	0.02	0	1.3±0.8	6	2.3±1.4	6	2.7±1.0	6
		8	1.0±0.0	6	1.3±0.5	6	1.0±0.0	6
		12			1.0±0.0	5		
Montipora sp.	0.01	0	3.7±0.9	12	3.8±0.4	12	3.7±0.5	12
		8	1.1±0.3	12	2.2±1.2	12	2.2±1.3	12
		12	1.1±0.3	10	1.4±0.5	12	1.6±1.0	11
		16	1.1±0.3	10	1.3±0.5	12	1.4±1.0	10
	0.02	0	3.5±0.8	6	3.3±1.0	6	4.0±0.0	6
		8	1.3±0.8	6	2.5±1.4	6	3.0±1.3	6
		12	1.2±0.4	6	2.6±1.1	5	2.3±1.2	6
		16	1.2±0.4	6	2.2±0.8	5	2.3±1.2	6
T. reniformis	0.01	0	3.2±1.2	12	2.7±1.4	9	2.7±1.4	9
		8	1.0±0.0	11	1.1±0.3	9	1.6±1.0	9
		12			1.0±0.0	9	1.0±0.0	8
	0.02	0	3.5±1.2	6	3.2±1.3	6	3.7±0.5	6
		8	1.2±0.4	6	1.3±0.5	6	1.2±0.4	6
		12	1.0±0.0	5	1.0±0.0	6	1.0±0.0	6

Those results suggest that longer period of incubation might help remaining a higher percentage of labelled–fragments over time. The concentration effect was only significant for fragments of *Montipora* sp. and was higher for clacein concentration of 0.02 g l^{-1} . Furthermore, for fragments of *P. damicornis* increasing the incubation time at lower calcein

Table 2. Growth rates (% of relative weight increase) of each species obtained 8, 12, and 16 weeks after incubations at each calcein concentration (C0: unlabelled control, C1: 0.01 g l^{-1} , C2: 0.02 g l^{-1}). Mean ± Standard deviation; n: sample size.

Species	Calcein groups	Initial weight (g)	n	% weight increase					
				8 weeks	n	12 weeks	n	16 weeks	n
S. pistillata	C0	3.2±0.6	6	25.0±11.8	6	66.3±25.7	6	111.6±40.8	6
	C1	5.2±1.6	36	31.7±13.0	36	65.9±23.3	34	116.4±46.1	34
	C2	6.2±3.0	18	24.7±13.4	18	54.7±29.1	17	92.9±52.9	17
S. caliendrum	C0	2.6±0.5	6	36.9±15.1	6	85.9±23.2	6	147.5±58.9	6
	C1	2.5±0.7	36	24.0±14.6	29	62.4±34.5	29	118.6±69.6	29
	C2	2.8±0.8	18	23.1±15.7	17	58.0±31.4	17	103.4±58.0	17
P. damicornis	C0	4.5±1.4	6	44.8±10.9	6	108.7±31.0	6	199.5±68.0	6
	C1	3.8±1.0	36	47.2±20.1	35	127.0±49.1	32	218.9±85.5	32
	C2	4.0±1.3	18	48.4±22.8	18	134.1±51.6	17	245.0±92.9	17
Echinopora sp.	C0	4.0±2.2	6	33.2±20.6	6	60.2±21.9	6	106.1±38.6	6
	C1	3.7±1.4	36	38.4±16.9	36	59.8±46.9	35	101.0±61.8	35
	C2	3.5±1.2	18	36.2±22.5	18	52.9±50.5	17	100.3±67.0	17
Montipora sp.	C0	4.5±1.3	6	47.6±16.6	6	89.9±17.4	6	156.8±12.8	6
	C1	3.3±1.2	36	52.3±31.7	36	91.3±28.6	33	142.0±64.0	33
	C2	3.3±1.5	18	49.0±21.4	18	69.4±49.9	17	129.7±76.7	17
T. reniformis	C0	8.7±2.1	6	19.6±11.9	6	26.5±13.9	6	42.7±12.4	6
	C1	7.0±3.9	30	13.7±8.7	29	29.1±15.3	27	47.1±21.1	27
	C2	6.4±3.2	18	11.7±8.0	18	24.4±14.5	17	39.3±22.0	17

concentration significantly helped in keeping the label visible over time ($p < 0.05$).

3.3. Effect of calcein on fragment growth

Fragments of each species showed an exponential growth over time, and their growth rates (% relative weight increase) obtained at the end of the study are reported in Table 2. Although the relative growth rates were observed to vary between species from 40 % (*T. reniformis*) to 200 % (*P. damicornis*), incubating fragments in calcein concentration of 0.01 g l^{-1} or 0.02 g l^{-1} did not significantly affect the growth rates of the fragments 8, 12, and 16 weeks following incubations (one–way ANOVA, $df = 2$, $p > 0.05$).

4. Discussion

4.1. On the importance of labelling in cultured corals

The live coral trade is worth about US$ 7,000 per tonne (WABNITZ *et al.*, 2003) and have mainly been focusing on fast growing branched species such as species of the genus Acropora, Pocillopora, Seriatopora, and Stylophora, (YATES and CARLSON, 1992). Improving culturing traded species in both *in situ* farms and *ex situ* aquarium and integrating standardised labelling methods for captive–bred or cultivated corals are likely to improve the conservation of coral reefs. Furthermore, cultivated corals would be more adapted to "aquarium conditions" compared to wild–caught corals (BORNEMAN and LOWRIE, 2001). The trial to test a practical protocol for which all scleractinian corals could be traded is one of the major and relevant issues in coral trade and represents a fair objective. Physical supports, plastic bud vases, and recycled plastic bottle lids fixed underneath a support have been used to trade cultivated coral colonies between aquarium centres (Van Dongen–Vogels, personal observations). Although these techniques appeared to be sensible enough for trading corals, to our knowledge, they still need to be standardised.

The method used in the present work

involves incubation or immersion of fragments of different scleractinian species into a calcein solution, hence the integration of a fluorescent complex during calcification of the fragments. The use of fluorochromes represents a relatively inexpensive and non detrimental method. For example, the estimate cost to label one coral fragment is less than 0.2 to 0.4 euros (in 2005). In addition, the ability to easily observe the fluorescent label in coral fragments (i.e. as easier as checking money notes under a UV lamp) and the fact that the calcein labelling method does not require unusual, specialized equipment nor timely analysis adds to the appeal of the approach

4.2. Optimal conditions and inter–species variation

In order to obtain labelled–fragments of six different cultivated scleractinian species, six different conditions of incubation were tested during this study. Although incubation at a calcein concentration of 0.01 g l^{-1} for at least 24 hours was sufficient to obtain 100 % of labelled –fragments of *S. pistillata, Montipora* sp., *S. caliendrum* and *P. damicornis*, incubation at a higher calcein concentration of 0.02 g l^{-1} for 36 hours resulted in 100 % of labelled–fragments of all species. MARSCHAL *et al.* (2004) showed that a 0.01 g l^{-1} calcein concentration were sufficient to stain octocoral skeleton, but in other taxa such as molluscs, higher calcein concentrations were required to obtain consistent fluorescent marks, e.g. 0.10 g l^{-1} (MORAN, 2000), 0.20 g l^{-1} (RUSSEL L and MEREDITH, 2000) and 0.50 g l^{-1} (KAELHER and MCQUAID, 1999). In any case, as shown here, longer incubation times (e.g. 24 or 36 hours compared to 12 hours) improved the efficiency and the durability of the label. Similar results were observed in BARNES (1970) who incubated corals into a 20 mg l^{-1} alizarin solution for 3 to 24 hours. In previous invertebrates studies, calcein incubation times tested varied on average from 3 to 55 hours (ILAN *et al.*, 1996), but a 24 hours period of incubation was appropriate for successful labelling (MORAN, 2000 : RUSSELL and MEREDITH, 2000 : RUSSELL and URBANIAK , 2004 : MARSCHAL *et al.*, 2004).

As calcein is incorporated in the aragonite skeleton during calcification, our results are reflecting the difference in calcification rates between coral species (GOREAU *et al.*, 1996 : GATTUSO *et al.*, 1999). The absence of a visible mark on some fragments immediately after calcein incubation also suggests that no or very little calcification occurred for those fragments during incubation (WILLENZ and HARTMAN, 1999). A potential weakness of using calcein in coral trade would be its relative lack of robustness over time. BASHEY (2004) observed that in *Poecilia reticulata* calcein marks can fade within 14 days when exposed to high temperatures or sunlight. Yet the observed decrease in the ability of detecting the marks within 8 to 16 weeks is believed to result from the addition of skeletal material on top of the calcein marks (BARNES, 1972). This would suggest that while the coral is incubated, the extension of the skeleton would result in the integration of the calcein and consequently in a visible mark on the skeleton of the fragment. However, as the thickening of the skeleton is occurring after its extension, the label will then appear undetectable. Therefore increasing the growth rate of the fragments during incubation (i.e. allowing both the growth and thickening of the coral skeleton) can be suggested in order to improve both the durability and efficiency of the labelling (DAY *et al.*, 1995 : DUVIVIER, 2006).

5. Conclusion and perspectives

We showed that the use of calcein can be a potential short–term, non–destructive tool in cultivated corals in trade over wild–caught ones. However, unsuccessful calcein labelling of *Lythophyton* sp. suggests that this method is inappropriate for soft corals (Van Dongen–Vogels, unpublished observations). An alternative labelling method may rely on the use of microchips which has proved to withstand in saline water up to 6 m depth. Moreover, once incorporated in the coral fragments of *S. caliendrum, Acropora* sp. and *Montipora* sp., the microchips was still easily read by a scanner after 3 months (DUVIVIER, 2006). This technique could be interesting in the long term but because of its relatively high cost, it is still difficult to implement it on a global scale. Further studies are then needed (i) to extend the

application of the calcein labelling method to a larger number of cultivated species, and (ii) to compare different potential labelling systems as well as evaluating the cost of these systems in the live coral trade market. International standardisation of the most efficient labelling system should ultimately be made and decided through proper international regulations.

Acknowledgements

We gratefully thank the Nausicaä Aquarium (Boulogne–sur–mer, France) for the use of their infrastructure and their coral species. We also thank L. Seuront for his constructive comments and criticism of this manuscript as well as one anonymous reviewer. This research was part of a Master thesis which was partially funded by the Catholic University of Louvain (Belgium).

References

BARNES, D.J. (1972): The structure and formation of growth–ridges in sceractinian coral skeletons. Proceedings of the Royal Society of London. Series B, Biol. Scie., **182**, 331–350.

BASHEY, F. (2004): A comparison of the suitability of alizarin red S and calcein for inducing a non lethally detectable mark in juvenile guppies. Notes. Trans. Am. Fish. Soc. **133**, 1516–1523.

BERNHARD, J.M., BLANKS, J.K., HINTZ, C.J. and T. CHANDLER (2004): Use of the fluorescent calcite marker calcein to label foraminiferal tests. J. Foraminifer. Res. **34**, 96–101.

BORNEMAN, E.H. and J. LOWRIE (2001): Advances in captive husbandry: an easily utilized reef replenishment means from the private sector? Bull. Mar. Sci., **69**, 897–913.

BRUCKNER, A.W. (2000): New threat to coral reefs: trade in coral organisms. Issues in S. and T., Fall, 1 –6.

BRUCKNER, A.W. (2001): Tracking the trade in ornamental coral reef organisms: the importance of CITES and its limitations. Aquarium Sci. Conserv., **3**, 79–94.

BRUCKNER, A.W. and E.H. BORNEMAN (2005): Developing a sustainable harvest regime for Indonesi a' s stony coral fishery with application to other coral exporting countries. Proc. 10th Int. Coral Reef Symp., Okinawa. In press.

DAY , R.W., WILLIAMS, M.C. and G.P. HAWKES (1995): A comparison of fluorochromes for marking abalone shells. Mar. Freshwat. Res., **46**, 599–605.

DELAHAYE , B. (2003): Croissance des coraux au Nausicaä. Rapport du Nausicaä, France.

DELBEEK, J.C. (2001): Coral farming: past, present and future trends. Aquarium Sci. Conserv., **3**, 171–181.

DODGE , R.E., WYERS, S., FRITH, H.R., KNAP, A.H., COOK, C., SMITH, R. and T.D. SLEETER (1984): Coral calcification rates by the buoyant weight technique: effects of alizarin staining. J. Exp. Mar. Biol. Ecol., **75**, 217–232.

DUVIVIER, M. (2006): Etude de la croissance et des marquages de trois espèces de coraux sclé ractiniaires en milieu artificiel (*Monitora* sp., *Seriatopora caliendrum* et *Acropora* sp.). Mémoire de licence, Université Catholique de Louvain (UCL), Belgique, 70 pp.

FABRICIUS, K.E. (2005): Effects of terrestrial runoff on the ecology of corals and coral reefs, review and synthesis. Mar. Poll. Bull., **50**, 125–146.

FOLKE, C., NYSTRöM, M. and F. MOBERG (2000): Coral reef disturbance and resilience in a human–dominated environment. TREE, **15**, 413–417.

GATTUSO, J.P., ALLEMAND, D. and M. FRANKIGNOULLE (1999): Photosynthesis and calcification at cellular, organismal and community levels in coral reefs: a review on interaction and control by carbonate chemistry. Am. Zool., **39**, 160–183.

GOMEZ , E.D., ALCALA A.C., YAP H.T., ALCALA L.C. and P.M. ALINO (1985): Growth studies of commercially important scleractinians. Proc. 5th Inter. Coral Reef Congr., Tahiti, **6**, 199–204.

GOREAU, T.J., GOREAU N.I., TRENCH, R.K. and R.L. HAYES (1996): Calcification rates in corals. Technical Comments. Sciences, **274**, 117.

GREEN, E. and F. SHIRLEY (1999): The global trade in corals. World Conservation Monitoring Centre. Biodiversity Series No. 10. World Conservation Press, Cambridge, UK. 70 pp.

GREEN, E.P. and H. HENDRY (1999): Is CITES an effective tool for monitoring trade in corals ? Coral Reefs, **18**, 403–407.

HANFEE, F. (1997): Traffic–India C/o WWF for Nature New Delhi. Chapter 21. Trade in Corals. In: Hoon, V. 1997. Proceedings of the Regional Workshop on the Conservation and Sustainable Management of Coral Reefs. Proc. No. 22, CRSARD, Madras.

HARRIOTT, V.J. (2002): Can corals be harvested sustainably? AMBIO: A Journal of the Human Environment, **32**, 130–133.

ILAN, M., AIZENBERG, J. and O. GILOR (1996): Dynamics and growth patterns of calcareous sponge spicules. Biol. Scie., **263**, 133–139.

ISHIHARA, A. (2000): WWF and TRAFFIC appeal to end illegal harvesting of native corals in Japan. TRAFFIC Dispatches, N°15. TRAFFIC East Asia –Japan.

KAEHLER, S. and C.D. MCQUAID (1999): Use of the fluorochrome calcein as an in situ growth

marker in the brown mussel *Perna perna*. Mar. Biol., **133**, 455–460.

LEIPS, J., BARIL, C.T., RODD, F.H., REZNICK, D.N., BASHEY, F., VISSER, G.J. and J. TRAVIS (2001): The suitability of calcein to mark poeciliid fish and a new method of detection. Trans. Am. Fish. Soc., **130**, 501–507.

MARSCHAL , C., GARRABOU, J., HARMELIN, J.G. and M. PICHON (2004): A new method for measuring growth and age in the precious red coral *Corallium rubrum* (L.). Coral Reefs, **23**, 423–432.

MORAN, A.L. (2000): Calcein as a marker in experimental studies newly–hatched gastropods. Mar. Biol., **137**, 893–898.

PETERSON, D., LATERVEER, M., VAN BERGEN. D., HATTA, M., HEBBINGHAUS, R., JANSE, M., JONES, R., RICHTER, U., ZIEGLER, T., VISSER, G. and H. SCHUHMACHER (2006): The application of sexual coral recruits for the sustainable management of *ex situ* populations in public aquariums to promote coral reef conservation –SECORE Project. Aquatic Conserv.: Mar. Freshw. Ecosyst., **16**, 167 –179.

RUSSELL, M.P. and R.W. MEREDITH (2000). Natural growth lines in echinoid ossicles are not reliable indicators of age, a test using *Strongylocentrotus droebachiensis*. American Microscopical Society, Inc. Invertebr. Biol., **119**,410–420.

RUSSELL, M.P. and L.M. URBANIAK (2004): Does calcein affect estimates of growth rates in sea urchins? Proc. of the 11th Inter. Echinoderm Conf. In: HEINZELLER, T., NEBELSICK, J.H. (Eds.), BALKEMA, A.A.. Rotterdam. In press. pp. 53–57.

SC50 DOC. 10. (2004): Convention sur le commerce International des Espèces de Faune et de Flore Sauvages menaces d' extinction. Cinquantième session du Comité permanant, Genève.

SHUMAN C.S., HODGSON G. AND R.F. AMBROSE (2004): Managing the marine aquarium trade: is eco–certification the answer? Envir. Conserv., **31**, 339–348.

TEO, J. (2005): Volunteers patrol park to stop illegal coral collectors. 26th January. Straits Times, Singapore.

THORROLD, S.R., JONES, G.P., HELLBERG, M.E., BURTON, R.S., SWEARER, S.E., NEIGEL, J.E., MORGAN, S.G., and R.R. WARNER (2002): Quantifying larval retention and connectivity in marine populations with artificial and natural markers. Bull. Mar. Scie., **70**, 291–308.

UNEP (2003): Convention and Coral Reefs. Fourteen multilateral environmental agreements, programmes, partnerships and networks relevant to the protection and conservation of coral reefs and the world summit on sustainable development plan on implementation. Produced by the UNEP Coral Reef Unit in collaboration with the WWF Coral Reefs Advocacy Initiative. 18 pp.

WABNITZ, C., TAYLOR, M., GREEN, E., and T. RAZAK (2003): From ocean to aquarium. Unpublished report, UNEP–WCMC, Cambridge, UK. URL http://www.unep–wcmc.org

WILKINSON, C., ed. (2004): Status of coral reefs of the world: 2004. Townsville, Australia: Australian Institute of Marine Science.

WILLENZ, PH. and W.D. HARTMAN (1999): Growth and regeneration rates of the calcareous skeleton of the Caribbean coralline sponge *Ceratoporella nicholsoni*, a long term survey. Memoirs of the Queensland Museum, Brisbane, **44**, 675–685.

YATES, K. and B. CARLSON (1992): Corals in aquarium: how to use selective collecting and innovative husbandry to promote reef conservation. Proc. of the 7th Inter. Coral Reef Symp., **2**, 1091–1095.

Received June 6, 2007
Accepted August 6, 2007

La mer 45 : 91-98, 2007
Société franco-japonaise d'océanographie, Tokyo

Numerical Radiative Transfer Simulations to Examine Influence of Shape of Scattering Phase Function of Suspended Particles on the Ocean Colour Reflectance

Takafumi HIRATA*,# and Gerald F. MOORE*,#

Abstract: Effects of shape of particle scattering phase function on the ocean colour reflectance are examined by means of radiative transfer simulations. The simulations suggest that different shape of particle phase function may cause 19% of discrepancy in the reflectance for oceanic waters, even if the backscattering probability of suspended particles does not change. The discrepancy can be even larger for absorbing waters in coastal zone.

Keywords: *Ocean Colour Reflectance, Phase Function Effects, Numerical Simulations*

1. Introduction

Numerical simulation of radiative transfer is a useful method to understand and predict variability of the ocean color reflectance from which biogeochemical properties of seawater may be exploited. When opticaliy shallow waters and inelastic scattering (including Raman scattering and fluorescence) are not considered, the time-independent simulations for 1D space (depth) are equivalent to solving the Equation of Radiative Transfer (ERT):

$$\left[\cos\theta\frac{d}{d\tau}+1\right]L(\Omega,\tau)=\omega\int 4\pi L(\Omega'\tau)P(\Psi,\tau)d\Omega' \quad (1)$$

where L and $d\Omega$'represent the radiance and infinitesimal solid angle, respectively. ω is the single scattering albedo and $P(\Psi,\tau)$ is the scattering phase function of seawater. If ω and P are given, the ERT can be solved with respect to L, provided initial and boundary conditions are given. From the solution of the ERT, the ocean colour reflectance can be obtained by R_{rs}= $L_u / \int_0^{2\pi} L\cos\theta_v\, d\Omega' = L_u / Ed$" where θ_v, L_u and E_d are the viewing zenith angle, the upward radiance (i.e. L (θ_v<90°) and the downward irradiance, respectively. Due to difficulties in measuring P, the classic measurements of P taken by PETZOLD (1972) have been assumed in the radiative transfer simulations for analysis of R_{rs}. Effects of this assumption should be evaluated prior to drawing final conclusions.

Only a few evaluations of the assumption exist. PLASS *et al.* (1985) showed that shape of phase function can significantly affect L_u. More recently however, MOBLEY *et al.* (2002) concluded that the exact shape of the phase function in backscattering directions is not critical if the backscattering probability is correct and a 10% of error is acceptable. Thus, results from the two groups do not agree well with each other, and re-examination is required. The objective of this paper is to re-evaluate the influence of the shape of P on R_{rs} by means of numerical simulations and to see whether the use of the single shape of P (i.e. PETZOLD P) is valid for different water types.

2. Simulations

The numerical radiative transfer simulations are made by Hydrolight (MOBLEY, 1995) for R_{rs}

*Centre for observation of Air-Sea Interactions and fluxes (CASIX)
#Plymouth Marine Laboratory, Prospect Place, The Hoe, Plymouth, Devon, PL1 3DH, UK
Corresponding author's Email: tahi@pml.ac.uk

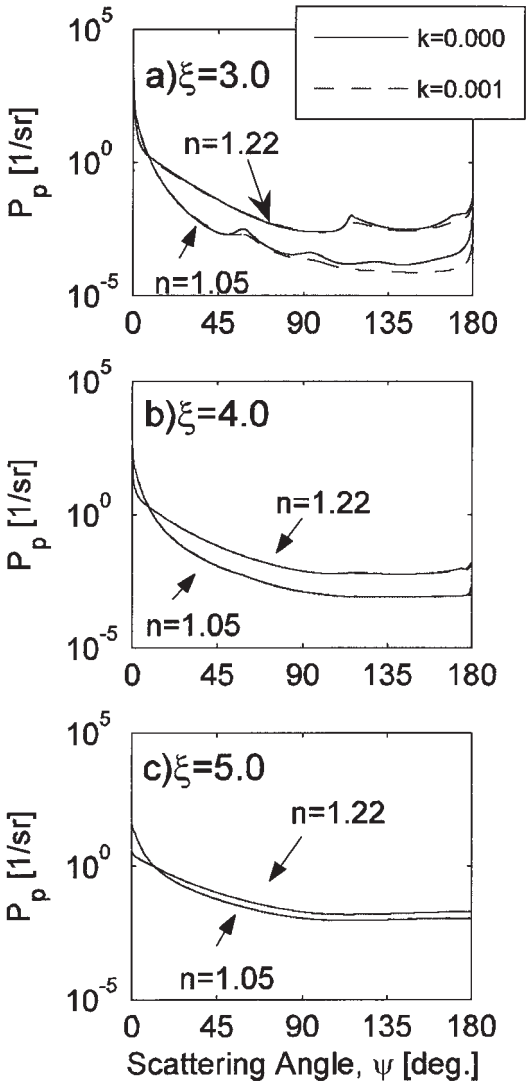

Fig. 1 Phase functions by Lorentz-Mie theory: (a) ξ =3.0 (b) ξ =4.0 and (c) ξ =5.0. Real and imaginary parts of the refractive index are represented by n and k, respectively.

using different shapes of P. The simulated R_{rs} is then compared. In the following, the justification for the phase functions used for the comparison is described.

2.1. Phase function, P

The phase function of seawater P is expressed by a weighted sum of that of pure seawater P_w and suspended particles P_p:

$$P = (1 - W)\, P_w + W P_p. \quad (2)$$

The weighting function W ($\equiv b_p/(b_w+b_p)$) explains a contribution of the particle scattering to the total scattering. Variations in P are caused by variations of P_w, P_p and W. Since variations in P_w are relatively much less than these in P_p and W, variations in P are determined by these in P_p and W in practice.

Due to the lack of sufficient measurements of P_p, Lorentz-Mie computations were performed just to obtain an idea of variability in P_p. In the Lorentz-Mie computations, particle size distribution $N(D)$ was varied according to Junge distribution $N(D) \sim D^{-\xi}$ where N and D represent number of particles and sphere-equivalent diameter of particles, respectively. Junge slope ξ was varied from 3.0 to 5.0. The complex refractive index (n) was varied from 1.05 to 1.22 for the real part to consider algal particles and mineral particles, and 0.0 to 0.001 for the imaginary part (k) to consider absorbing particles. The computations show that the shape of P_p is remarkably variable at small and large angles (Fig. 1). According to GORDON (1993) however, the scattering at the small scattering angles has little effect on the light field. Hence we focus on P_p at large angles, or backscattering angles. The P_p at backscattering angles predicted by Lorentz-Mie theory may be classified into three classes: (I) P_p with a peak at around 180° of scattering angle (Fig. 1a), (II) P_p with no such peak (Fig. 1c) and (III) the intermediate case (Fig. 1b). In order to examine possible maximum effects of phase function on the ocean colour reflectance, two boundary shapes of P_p (i.e. backward-peaked and non-backward-peaked phase functions) are considered.

2.2.1 Backward-peaked phase function of suspended particles

The backward-peaked P_p obtained from Lorenz-Mie computations (Fig. 1a) has a similar shape to that of PETZOLD phase function (shown as a bold curve in Fig. 2) which has a remarkable peak at backward direction. Because the aim of this paper is to examine effects of use of the PETZOLD P_p in ocean colour analysis, the PETZOLD P_p is used here as a reference phase function that represents the backward-peaked P_p at the same time.

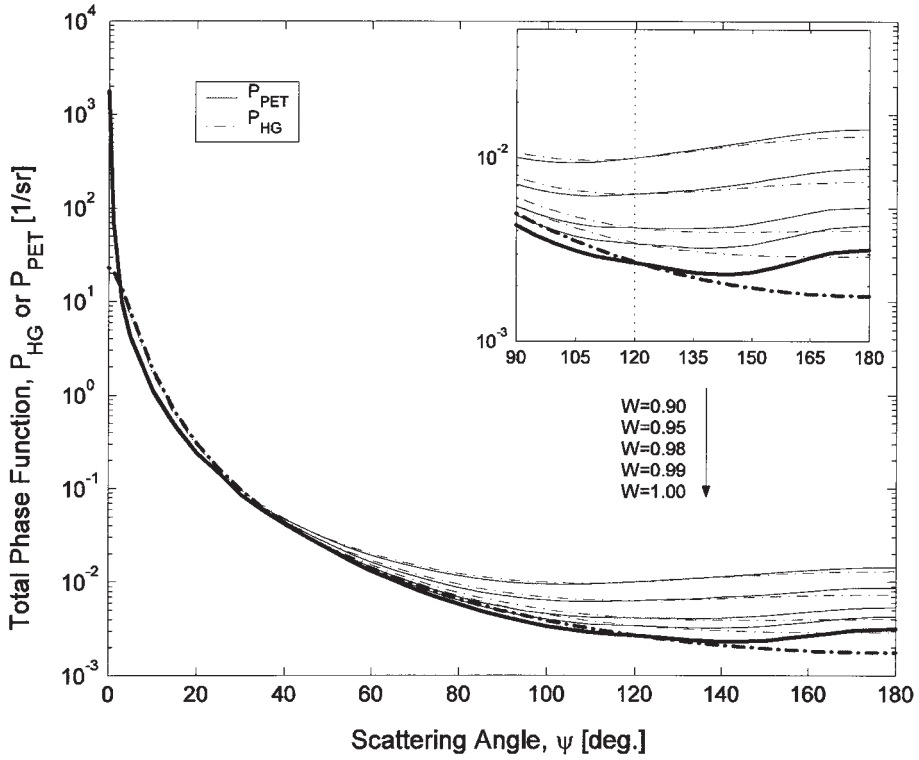

Fig. 2 Total phase function calculated with particle phase function represented by Heyney-Greenstein phase function P_{HG} (dash-dot curves) and PETZOLD phase function P_{PET} (solid curves). From the top to the bottom, W ($=b_b/b_{tot}$) varies from 0.90 to 1.00. Thick curves represent P_{HG} and P_{HG} for W=1.0, or P_{pHG} and P_{pPET} respectively. Subplot is drawn to emphasize the phase functions at the backscattering angle (i.e. $90 \leq \phi \leq 180$).

2.2.2 Non-backward-peaked phase function

The other characteristic shape of P_p predicted from Lorentz-Mie theory has a relatively flat shape in backward scattering angles (i.e. Non-backward-peaked phase function, Fig. 1c). Henyey-Greenstein phase function P_{pHG} represents such a shape:

$$P_{pHG} = \frac{1}{4\pi} \frac{1-g^2}{[1+g^2-2g\mu]^{3/2}} \qquad (3)$$

where g and μ represent the asymmetry factor and cosine of scattering angle. Fig. 2 shows that P_{pHG} (shown as P_{HG} for W=1.0) is similar to the non-backward-peaked P_p predicted by Lorenz-Mie theory shown in Fig. 1c. We use P_{pHG} here to represent the non-backward-peaked P_p, rather than those determined by Lorentz-Mie theory, because P_{pHG} is expressed in an analytical form so that P_p can readily be assigned the same backscattering fraction b_{bp}/b_p as that of PETZOLD P_p. Resultant g used here is 0.9185.

2.2.3 The phase functions of total water

Variations of P calculated with P_{pPET} and P_{pHG} are shown in Fig. 2 for W varying from 0.9 to 1.0. For W=1.0 (bold curves), P is simply either P_{pPET} (solid) or P_{pHG} (dash-dot): see Eq. 2, too. It is seen that shape of backward P calculated from P_{pPET} or P_{pHG} are different only when W exceeds 0.9 due to the large contribution of P_w at W<0.9. P_{HG} has been used to represent P for total (water + particle) seawater, and such approximation is not adequate for oceanic waters (HALTRIN, 2002). However, P_{HG} is used here for an approximation to P_p, not to P. In addition, P_{HG} used as P_p still preserves a physical phenomenon that total P obtained from P_{pHG} has the least variability at the scattering angle of 120 deg. (OISHI, 1990) (see inset of Fig. 2).

Thus, P_{HG} would still be useful for oceanic application as long as it is used as one of the boundary shape of P_p.

2.3. Other input parameters

The radiative transfer simulations require not only P but also the single scattering albedo $\omega = b_{tot} / (a_{tot}+b_{tot})$ as well as initial and boundary conditions. ω is calculated from a_{tot} and b_{tot} which are determined as follows. The absorption coefficient is decomposed into that by pure water (a_w) and by any other substances (a_{py}) so that $a_{tot}=a_w+a_{py}$. Subscript py means particle plus yellow substance. Due to lack of sufficient measurements to define natural variability of a_{py} in the world oceans, a_{py} is numerically varied from 0 to 1.59 m^{-1}; this range of values covers the maximal a_{py} observed in coastal waters by BABIN *et al.* (2003a). Effects of the upper limit chosen will be discussed in Section 3.2. Values of a_w are taken from a measurement made by POPE and FRY (1997). The scattering coefficient may also be decomposed into $b_{tot}=b_w+b_p$ where subscript p means particles. Due to the same reason as a_{py} above, b_p is numerically varied from 0 to 7.37 m^{-1}; such a value of scattering corresponds to a sediment load of 7 to 15 g/m^{-3} (BABIN *et al*, 2003b) and the maximum CHL considered here Selection of the upper limit of b_p will also be discussed in Section 3.2. Values of b_w are taken from MOREL (1974). Table 1 summarizes values of a_{py} and b_p used in the present simulations.

The initial condition to the ERT is determined from HARRISON and COOMBES (1988) and GREGG and CARDER (1990) with variable solar zenith angle (θ_s) from 0 to 75 deg. as shown in Table 1 (Results are shown only up to 58.3 deg. within the geometry for remote sensing, which does not affect a conclusion drawn in this paper). The boundary condition to the ERT is determined from Cox-Munk wave distribution with the wind speed of 7.2 m/s. The ocean is assumed to be optically deep. Actual simulations are performed for 15 discrete optical depths from τ =0 down to τ =7 with 0.5 interval, although we only focus on τ =0 which is relevant remote sensing applications. Wavelength λ is selected based on SeaWiFS bands (Table 1) but restricted to shorter wavelengths to minimise effects of inelastic scattering, including Raman scattering and fluorescence. The simulations are performed for all possible combinations of input parameters above (including any combination between a_{tot} and b_{tot}). Radiance to derive R_{rs} is obtained from 0 to 49° of the viewing zenith angle and from 0 to 180° of the viewing azimuth angles (Table 1).

Table 1 Parameter values used for the simulations. All combinations of the parameters are considered in the simulations. Wavelengths larger than 555 nm are not considered to minimise possible effects of inelastic scattering.

a_{py} [m^{-1}]	b_p [m^{-1}]	Solar zenith angle [deg.]	Viewing zenith angle [deg.]	Viewing azimuth angle [deg.]	Wavelength [nm]
0.000	0.000	0.0	2.0	0	412.5
0.017	0.019	8.3	7.0	15	442.5
0.028	0.038	16.7	13.0	30	490.0
0.046	0.073	25.0	19.0	45	510.0
0.076	0.140	33.0	25.0	60	555.0
0.126	0.271	41.7	31.0	75	
0.209	0.525	50.0	37.0	90	
0.347	1.017	58.3	44.0	105	
0.576	1.967	66.7	49.0	120	
0.956	3.807	75.0	55.0	135	
1.587	7.368		61.0	150	
			67.0	165	
			73.0	180	
			79.0		
			85.0		

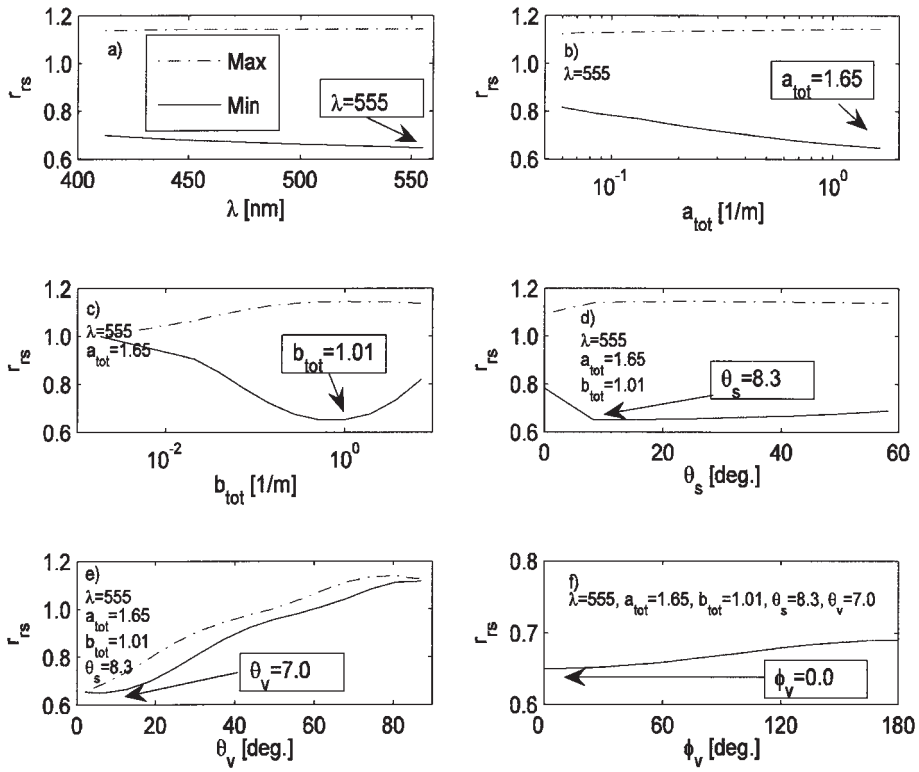

Fig. 3. Maximum and minimum values of r_{rs} ($=R_{rsHG}$ / R_{rsPET}): (a) as a function of only λ. All of range of other parameters is considered; (b) as a function of only a_{tot} but λ is fixed at 555 nm; (c) as a function of b_{tot} at λ =555 nm and at a_{tot} =1.65 m^{-1}; (d) as a function of θ_s at λ =555 nm, a_{tot} =1.65 m^{-1}, and b_{tot} =1.01 m^{-1}; (e) as a function of θ_v at λ =555 nm, a_{tot} =1.65 m^{-1}, b_{tot} =1.01 $m^{-1}$and θ_s=8.30°; (f) as a function of ϕ v at λ =555 nm, a_{tot} =1.65 m^{-1}, b_{tot} =1.01 m^{-1}, θ_s=8.30° and θ_v=7.00°.

3. Results and discussions

The influence of P may be described by the ratio between R_{rs} simulated with P_{pPET} (denoted by R_{rsPET} hereafter) and R_{rs} simulated with P_{pHG} (R_{rsHG}): i.e. $r_{rs} = R_{rsHG}/R_{rsPET}$. The influence of P_p is shown by the deviation of r_{rs} from unity, and the largest influence can be evaluated by either of the maximum or minimum value of r_{rs}.

3.1 Estimation of the largest influence

Fig. 3a depicts r_{rs} as a function of only λ. All other variables, such as inherent optical properties (i.e. a_{tot} and b_{tot}, or ω) and viewing and illumination angles, were varied. The maximum value of r_{rs} ($\approx$1.16) is almost independent of λ. The minimum values of r_{rs} decreases from 0.70 to 0.65 as λ increases. Since deviation of the minimum r_{rs} from unity is larger than deviation of maximum r_{rs} from unity at all λ, the maximum discrepancy between R_{rsHG} and R_{rsPET} is represented by the minimum r_{rs}. The largest influence of P_p is found at λ =555 nm.

Fig. 3b shows r_{rs} as a function of only a_{tot} but wavelength is now fixed at 555 nm. All other variables except λ are allowed to vary. The maximum values of r_{rs} are almost constant while the minimum values of r_{rs} decrease with a_{tot}. Since the greatest deviation of the minimum r_{rs} from unity is larger than that of maximum r_{rs}, the largest influence of P_p is found by the minimum r_{rs} at a_{tot}=1.65 m^{-1}.

Fig. 3c shows r_{rs} as a function of only b_{tot} but now λ and a_{tot} are fixed at 555 nm and 1.65 m^{-1}, respectively. Variation of the minimum r_{rs} is not monotonic. It firstly decreases and then increases, as b_{tot} increases. Since the greatest deviation of the minimum r_{rs} from unity is larger than that of maximum r_{rs}, the largest

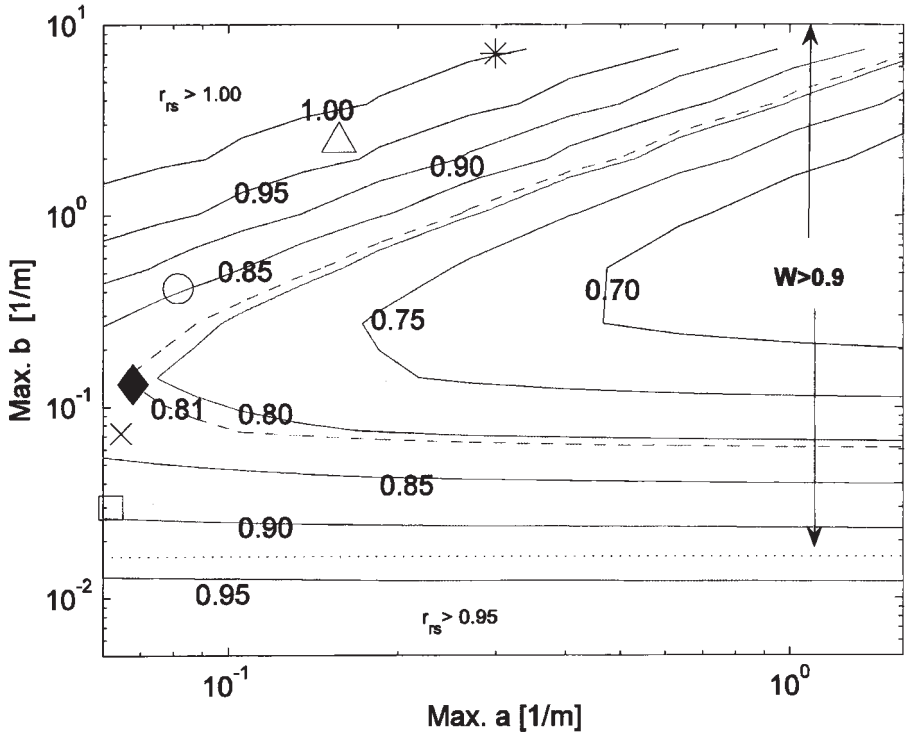

Fig. 4 Contour plot of r_{rs} as a function of upper limits of a_{tot} and b_{tot}. Chlorophyll a concentrations are specified by: □ =0.03, × =0.10, ◆=0.22, o=1.00, Δ=10.0, ＊=40.0mg/m^{-3}. Dotted line shows a boundary for W>0.9. Dashed curve is drawn especially for r_{rs} =0.81.

influence of P_p occurs at b_{tot}= 1.01 m^{-1}.

r_{rs} at λ =555 nm, a_{tot}=1.65 m^{-1} and b_{tot}=1.01 m^{-1} is shown in Fig. 3d as a function of solar zenith angle θ_s. The largest influence of P_p is found when θ_s=8.30 deg. Fig. 3e shows r_{rs} at λ =555 nm, a_{tot}=1.65 m^{-1}, b_{tot}=1.01 m^{-1} and θ_s =8.30 deg. as a function of the viewing zenith angle θ_v, in which the largest influence is found at θ_v=7.00 deg. Finally ϕ_v at which the largest influence of phase function is found is 0 deg, in which case r_{rs}=0.65. (Fig. 3f).

The largest influence of particle phase function is found at λ =555 nm, a_{tot}=1.65 m^{-1}, b_{tot} =1.01 m^{-1}, θ_s=8.30 deg., θ_v=7.00 deg., and ϕ_v= 0 deg. with r_{rs} =0.65, indicating that the influence of P_p can be significant to cause 35%=100 (1−0.65) of maximum discrepancy in R_{rs} according to the present simulations.

3.2 Effects of choice in upper limit of a_{tot} and b_{tot}

In the results shown above, the largest influence of P_p was found at a_{tot}=1.65 m^{-1} which is the upper limit of a_{tot} set in our simulations. Also the largest influence of phase function as a function of b_{tot} did not show a constant effect over b_{tot}. These mean that our results obtained earlier depend on the choise of the upper limit of a_{tot} and b_{tot}, or equivalently a_{py} and b_p since a_w and b_w are regarded as constants. for each waveleugth In order to see effects of this choice, simulations are repeated by changing the upper limit of a_{tot} and b_{tot} (denoted hereafter by Max a_{tot} and Max b_{tot}, respectively). Fig. 4 shows the largest influence of P_p in terms of r_{rs}, as functions of Max a_{tot} and Max b_{tot}. If Max a_{tot} assumed in simulations is larger / smaller than "real" upper limit of a_{tot}, the largest influence of phase function is over/under-estimated when Max b_{tot} is relatively large. When Max b_{tot} is relatively small however, the over/under estimation is less severe or even negligible, even if Max a_{tot} is incorrectly selected. This is consistent with Section 2.2.3 that the phase function

effects are remarkable only when W>0.9.

If Max b_{tot} assumed is relatively larger/smaller than actual upper limit of b_{tot} the largest influence of P_p simulated is over/under-estimated, when the magnitude of actual b_{tot} is small. When the magnitude of actual b_{tot} itself is large however, the largest influence of P_p simulated will be under/over-estimated if Max b_{tot} assumed is relatively larger/smaller than actual upper limit of b_{tot}. The above results indicate that precise determination of the upper limit of a_{tot} and b_{tot} is required for quantitative prediction of the influence of P_p.

MOREL and MARITORENA (2001) proposed statistical relationships between a_{tot} (or b_{tot}) and Chlorophyll a concentration (CHL) for oceanic water based on numerous in situ observations, from which natural Max a_{tot} and Max b_{tot} may be determined in terms of an upper limit of CHL since the statistical relationship is non-linear but monotonic. Their data showed nearly 40 mg m^{-3} of the maximum CHL in oceanic waters: see their Fig.3 in MOREL and MARITORENA (2001). Thus, realistic Max a_{tot} and Max b_{tot} can be calculated for oceanic water by using CHL=40 mg m^{-3}. The largest influence of P_p estimated using Max a_{tot} and Max b_{tot} derived in this way are shown in Fig. 4 as a star symbol. The largest influence of P_p for CHL=0.03, 0.1, 1.0 and 10.0 mgm^{-3} are also superimposed for comparison as well as for CHL=0.22 mg m^{-3} which is a global annual average of CHL derived from SeaWiFS. When CHL is 0.22 mg m^{-3}, r_{rs} is 0.81 showing that 100 (1.00-0.81) =19 % of largest influence of P_p. The influence is relatively less for lower and higher CHL. The present result suggests that the influence of P_p on R_{rs} (or equivalently L_u) can be significant for oceanic waters.

For coastal waters, a significant number of observations for a_{tot} and b_{tot} are required to define their maximum variability. Therefore quantitative prediction of the phase function effects cannot be made for coastal waters at the present stage. However, general tendency of the effects for coastal waters can be found at least qualitatively (Fig. 4). For absorbing waters (e.g. Baltic sea) where Max a_{tot} is much larger than that for oceanic waters, the possible largest influence of P_p on R_{rs} will be larger than that for oceanic waters, unless Max b_{tot} (or b_{tot}) is also much larger than b_{tot} for oceanic waters. For scattering waters (e.g. Black sea) where Max b_{tot} is much larger, the largest influence of P_p on R_{rs} will be reduced unless Max a_{tot} is also much larger.

It is clear that a balance between the absorption and scattering play a significant role in the phase function effects, and the absorbing water or scattering waters may be defined based on ω. However, it should be emphasized that absolute magnitude of b_{tot} (or alternatively b_p) must also be considered together with ω when the phase function effects are estimated, since (1) we saw in Section 2.2.3 that significant difference in P is found only at W >0.9 and (2) a value of ω cannot specify a unique value of W.

Phase function effects for the absorbing waters implies that, even for oceanic waters, the effects can be significant at near-infrared wavelengths where the absorption by pure seawater itself is much larger than that at visible wavelengths. The near-infrared has a particular importance for atmospheric correction scheme of the ocean colour imagery, especially when the waters have a significant reflectance in the NIR; the bright pixel assumption (MOORE *et al*, 1999). Thus, the present work implies that the phase function effects need to be considered in remote sensing application.

5. Conclusion

The largest influence of P_p is estimated to be 19% for oceanic waters. For coastal waters, the influence can even be larger in absorbing waters, whereas it can be smaller in scattering waters. The influence of shape of phase function of suspended particles can be significant, especially when intensity of scattering of particle is large enough compared to that of pure seawater (0.9<W). The present results suggest that the shape of P has to be taken into account in the ocean colour analysis, especially in highly absorbing waters.

Acknowledgements

This work was a part of Project 4 “Biogeochemistry of the Open Ocean” in Science Element 2 “Biogeochemistry of the Upper Ocean”

by Centre for Air-Sea Interactions and fluxes (CASIX): CASIX publication number 43. The authors acknowledge financial support from Natural Environmental Research Council (NERC).

References

BABIN, M., D. STRAMSKI, G. M. FERRARI, H. CLAUSTRE, A. BRICAUD, G. OBOLENSKY and N. HOEPFNNER (2003a): Variations in the light absorption coefficients of phytoplankton, nonalgal particles, and dissolved organic matter in coastal waters around Europe, J. Geophys. Res., **108** (C7), 3211, doi:10.1029/2001JC000882.

BABIN, M., A. MOREL, V. FOURNIER-SICRE, V. FELL, D. STRAMSKI (2003b): Light scattering properties of marine particles in coastal and open ocean waters as related to the particle mass concentration. Limnol. Oceanogr., **48**, 843–859.

GORDON, H. R. (1993): Sensitivity of radiative transfer to small-angle scattering in the ocean: Quantitative assessment, Appl. Opt., **32**, 7505–7511.

GREGG, W. W. and K. L. CARDER (1990): A simple spectral solar irradiance model for cloudless maritime atmospheres, Limnol. Oceanogr., **35**, 1657–1675.

HARRISON, A. W. and C. A. COOMBES (1988): An opaque cloud cover model of sky short wavelength radiance, Solar Energy, **41**, 387–392.

HALTRIN, V. I. (2002): One-parameter two-term Henyey-Greenstein phase function for light scattering in seawater, Appl. Opt., **41**, 1022–1028.

MOBLEY, C. D. (1995): Hydrolight 3.0 User's Guide. SRI International, California.

MOBLEY, C. D., L. K. SUNDMAN and E. BOSS (2002): Phase function effects on oceanic light fields, Appl. Opt., **41**, 1035–1050.

MOORE, G. F., J. AIKEN and S. J. LAVENDER (1999): The atmospheric correction of water colour and the quantitative retrieval of suspended particulate matter in Case II waters, Int. J. Remote Sensing, **20**, 1713–1733.

MOREL, A. (1974): Optical properties of pure water and pure seawater, *In* Optical aspects of Oceanography, N.G.Jerlov and E.Steemann Nielsen (Eds.), Academic, New York, p.1–24.

MOREL, A. and S. MARITORENA (2001): Bio–optical properties of oceanic waters: A reappraisal, J. Geophys. Res., **106**, 7163–7180.

OISHI, T. (1990): Significant relationship between the backward scattering coefficient of sea water and the scatterance at 120°, Appl. Opt., **29**, 4658–4665.

PETZOLD, T. J. (1972): Volume scattering function for selected ocean waters SIO Ref.72–78, Scripps Inst. of Oceanogr., Univ. of California, San Diego.

PLASS, G. N., G. W. KATTAWAR and T. J. HUMPHREYS (1985): Influence of the oceanic scattering phase function on the radiance, J. Geophys. Res., **90**, C2, 3347–3351.

POPE, R. M and E. S. FRY (1997): Absorption spectrum (380–700nm) of pure water, Appl. Opt., **36**, 8710–8723.

Received March 8, 2007
Accepted August 9, 2007

La mer 45 : 99, 2007
Société franco-japonaise d'océanographie, Tokyo

資　料

第 45 巻第 2 号掲載欧文論文の和文要旨

神田穣太[1]、伊藤貴行[2]、野村規宗[2]：北太平洋および東シナ海表層における低濃度硝酸塩の鉛直分布

北太平洋および東シナ海の表層において化学発光法による高感度分析法を用いて低濃度硝酸塩の測定を行った。狭い採水深度間隔で得られた鉛直分布から、有光層内では硝酸塩濃度は概ね一様であり、濃度躍層の上端以深で急激に濃度が上昇することが示された。濃度躍層より上層では硝酸塩濃度は3.1〜96.2 nMの範囲であり、これらの濃度は下層からの硝酸塩供給を反映して変動していると推定された。濃度躍層上端の深度は、混合層がより深くまで達していた 2 測点を除いて相対光強度0.58–3.5%の範囲にあった。これらの深度は一般的な有光層の下端とほぼ対応しており、生物による硝酸塩同化によって決まっていることを示唆している。観測された硝酸塩濃度の鉛直分布が定常的に維持されると仮定した場合、濃度躍層上端付近のごく狭い深度範囲で硝酸塩の正味の消費があり、有光層上部では正味の消費・生成はないことが示唆された。

([1] 東京海洋大学海洋科学部　〒108–8477 東京都港区港南4–5–7；[2] 静岡大学理学部　〒422–8529 静岡市駿河区大谷836；連絡先　〒108–8477 東京都港区港南4–5–7　東京海洋大学海洋科学部　神田穣太　E-mail: jkanda@kaiyodai.ac.jp)

Virginie Van Dongen-Vogels* and Jérôme Mallefet：Fluorescent labelling of cultivated corals as a sustainable management tool in coral trade and reefs conservation

六放サンゴ類は、利潤のあがる商品として重要であり、従来は主として天然のものが対象とされてきた。天然個体群への圧力軽減のために商業的取引の規制強化および水槽での無性的/有性的再生産の取り組みを実施するにあたっては、サンゴの出自（養殖か天然か）を確かめるための標識手法が求められよう。そこで我々は、2 型の成長様式（枝状か葉状）の養殖サンゴ 6 種から得た81の断片を用いて、カルセインを加えた培養による簡便な標識法を試験した。標識に最適の条件を調べるために、2 通りのカルセイン濃度（0.01および0.02 g・L^{-1}）と 3 通りの培養時間（12、24および36h）を設定した。サンゴ断片上の標識の視認性は、培養後 8 、12および16週間に評価された。カルセイン培養された*S. caliendrum, Echinopora* sp., *T. reniformis, P. Damicornis,* および*S. pistillata*と*Montipora* sp.の断片について、それぞれ59、61、79、96および98%が首尾よく標識されていた。標識の質と耐久性は、種により異なったけれども、いづれも培養時間が最長の場合に最良であった（2 通りのカルセイン濃度のどちらでも）。培養サンゴの標識にこのカルセイン法が適切であることが、他の標識法と比較して、またサンゴの商業的利用の持続的管理およびサンゴ礁の保全と関連して議論される。

(Laboratory of Marine Biology, Catholic University of Louvain (UCL), Batiment Kellner, 3 Place Croix du Sud, 1348 Louvain-La-Neuve, Belgium)

Takafumi Hirara*,# and Gerald F. Moore*,#: Numerical radiative transfer simulations to examine influence of shape of scattering phase function of suspended particles on the ocean color reflectance

海洋懸濁粒子による可視光一次散乱角度分布が、どれほど海洋の可視光反射スペクトルに影響を与えるのかを見積もるために、海中放射伝達の数値シミュレーションを行った。懸濁粒子による後方散乱率がたとえ同じであると仮定しても、後方拡散の角度分布が異なれば外洋の可視光反射スペクトルは最大19%異なりえることが示された。この相違は、可視光の吸収が散乱より比較的強いと特徴付けられる海域では、さらに増大する。

(*Centre for observation of Air-Sea Interactions and fluxes (CASIX),# Plymouth Marine Laboratory, Prospect Place, The Hoe, Plymouth, Devon, PL1 3DH, UK. Corresponding author's Email: tahi @pml.ac.uk)

La mer 45 : 100, 2007
Société franco-japonaise d'océanographie, Tokyo

学　会　記　事

1．2006年 8 月25日　日仏会館で特別講演会の夕べが開かれた。

2．2006年12月 7 日（火）　日仏会館（511号室）で幹事会が開催された。

審議事項

1．フランスから農林水産技師：ソフィー　ビオッシュ（Sylvain Pioch）女史が来年 1 ～ 3 月　東大・小松研究室へ留学予定であったが、交流協定などもあり水工研（波崎）へ交渉中である。滞在中には本学会が支援する提案が了承された。

2．学会活性化のための会則の見直しなどに関して会長から事情説明があり、早急に会則などの原案を作成することを確認した。

3．学会賞受賞委員会の活動に関して審議し、会長が会則通り13名を指名し、評議員の可否の投票で決定する手続きを行うときめた。

指名委員：荒川　久幸　磯田　　豊　奥田　邦明
神田　穣太　北出裕二郎　河野　　博
小林　雅人　小松　輝久　桜本　和美
千手　智晴　田中　祐志　前田　昌調
吉田　次郎

4．Francois Simard氏が訪日の挨拶をした。

3．2007年4月（10日火）日仏会館（511号室）で幹事会が開催された。

審議事項

1．平成19年度総会・学術研究発表会は 6 月 9 日（土）日仏会館で開催することに決めた。評議員会の開催は当日の昼休みとする。

2．学会の会則の見直しについて
　評議員数や表彰規定などは現在の学会の体制に適合するように見直し、総会に改正案を諮ることに下。

3．評議員会へ提出する議案について下記のように決定した。
H19年度　事業（案）
1．総会　学術研究発表会　幹事会　開催
2．学会の会則の見直し
3．La mer　発刊

4．学会賞のメダルの変更については、製作者に以前のメダルと模倣した作品を格安（一個：1万円程度）でお願いすることに決めた。

4．受贈図書
東海大学紀要海洋学部　Vol.4（1,2),
高知大学海洋研究報告　No. 24
水産総合研究センターNo. 6
潮音　No. l
FRAニュース　Vol. 8,9
東京大学海洋研究所　ニュースレター　No. 13–15
国立科学科学博物館専報　第40–42号
神奈川県立博物館研究報告　36号
なっしま　No. 29–39
農業工学研究所研究成情報18年度
農工研ニュース　Vol. 44–48
NII News No. 15, 16
RESTEC 57. 58. 59号
Ocean Science Journal Vol. 42 No. 2
Bulletin of the National Science Museum Vol. 32 No. 2

賛 助 会 員

アレック電子株式会社	神戸市西区井吹台東町７－２－３
株式会社 イーエムエス	神戸市中央区東川崎町１－３－３ 神戸ハーバランドセンタービル　13F
有限会社 英和出版印刷	文京区千駄木４－20－６
株式会社 内田老鶴圃 内田　悟	文京区大塚３－34－３
財団法人 海洋生物環境研究所	千代田区神田神保町３－29　帝国書院ビル５Ｆ
株式会社 川合海苔店	大田区大森本町２－31－８
ケー・エンジニアリング株式会社	台東区浅草橋５－14－10
いであ株式会社	世田谷区駒沢３－15－１
三洋測器株式会社	渋谷区恵比須南１－２－８
株式会社高岡屋	台東区上野６－７－22
テラ株式会社	文京区湯島４－１－13－402
渡邊機開工業株式会社	愛知県渥美郡田原町神戸大坪230

日仏海洋学会入会申込書

（正会員・学生会員）

	年度より入会	年　月　日申込
氏　名 ローマ字		年　月　日　生
住　所　〒 勤務先　機関名 電　話　E-mail:		
自　宅　住　所　〒 電　話　E-mail:		
紹介会員氏名		
送付金額　円	送金方法	
会誌の送り先（希望する方に○をつける）	勤務先　自　宅	

（以下は学会事務局用）

受付	名簿 原簿	会費 原簿	あて名 カード	学会 記事

入会申込書送付先：〒150-0013 東京都渋谷区恵比寿 3-9-25

（財）日仏会館内

日 仏 海 洋 学 会

郵便振替番号：00150−7−96503